AD NUMBER

ADB015026

LIMITATION CHANGES

TO:

Approved for public release; distribution is unlimited.

FROM:

Distribution authorized to U.S. Gov't. agencies only; Test and Evaluation; FEB 1976. Other requests shall be referred to Air Force Avionics Lab., Wright-Patterson AFB, OH 45433.

AUTHORITY

AFAL ltr 17 Sep 1979

AFAL-TR-76-57

THREE TO FIVE MICRON LASER INVESTIGATION

UNITED TECHNOLOGIES RESEARCH CENTER
EAST HARTFORD, CONNECTICUT 06108

SEPTEMBER 1976

FINAL REPORT FOR PERIOD JANUARY 1975 - DECEMBER 1975

AIR FORCE AVIONICS LABORATORY
AIR FORCE WRIGHT AERONAUTICAL LABORATORIES
AIR FORCE SYSTEMS COMMAND
WRIGHT-PATTERSON AIR FORCE BASE, OHIO 45433

NOTICE

When Government drawings, specifications, or other data are used for any purpose other than in connection with a definitely related Government procurement operation, the United States Government thereby incurs no responsibility nor any obligation whatsoever; and the fact that the Government may have formulated, furnished, or in any way supplied the said drawings, specifications, or other data, is not to be regarded by implication or otherwise as in any manner licensing the holder or any other person or corporation, or conveying any rights or permission to manufacture, use, or sell any patented invention that may in any way be related thereto.

This report has been reviewed and is approved for publication.

O. P. Breaux
Mr. O. P. Breaux
Project Engineer

R. F. Paulson
Dr. R. F. Paulson, Actg Chief
E-O Sources Group

FOR THE COMMANDER

Edwin B Champagne
Dr. E. B. Champagne, Acting Chief
Electro-Optics Technology Branch

Copies of this report should not be returned unless return is required by security considerations, contractual obligations, or notice on a specific document.

AIR FORCE - 22 OCTOBER 76 - 100

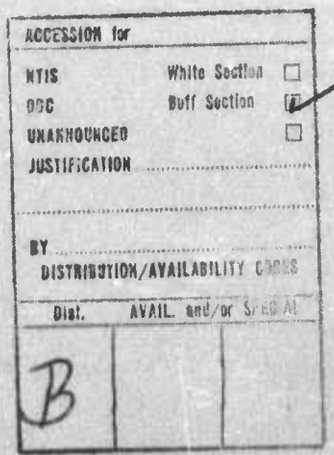

Unclassified

SECURITY CLASSIFICATION OF THIS PAGE (When Data Entered)

REPORT DOCUMENTATION PAGE

READ INSTRUCTIONS BEFORE COMPLETING FORM

1. REPORT NUMBER: AFAL-TR-76-57	2. GOVT ACCESSION NO.
3. RECIPIENT'S CATALOG NUMBER	
4. TITLE (and Subtitle): THREE TO FIVE MICRON VET LASER INVESTIGATION	5. TYPE OF REPORT & PERIOD COVERED: Final Report 1/2/75-12/31/75
6. PERFORMING ORG. REPORT NUMBER: UTRC-R75-952051-13	
7. AUTHOR(s): John A. Shirley	8. CONTRACT OR GRANT NUMBER(s): F33615-75-C-1047 NEW
9. PERFORMING ORGANIZATION NAME AND ADDRESS: United Technologies Research Center, East Hartford, CT 06108	10. PROGRAM ELEMENT, PROJECT, TASK AREA & WORK UNIT NUMBERS: 2001-01-35 62204F AF 4L
11. CONTROLLING OFFICE NAME AND ADDRESS: Air Force Avionics Laboratory (DHO-1), Air Force Systems Command, Wright-Patterson AFB, OH 45433	12. REPORT DATE: Sept 1976
	13. NUMBER OF PAGES: 50
14. MONITORING AGENCY NAME & ADDRESS (if different from Controlling Office): Final rept. 2 Jan – 31 Dec 75, 58p.	15. SECURITY CLASS. (of this report): Unclassified
	15a. DECLASSIFICATION/DOWNGRADING SCHEDULE

16. DISTRIBUTION STATEMENT (of this Report)

Distribution limited to U. S. Government agencies only; test and evaluation results reported; (February 1976). Other requests for this document must be referred to AFAL/DHO, WPAFB, OH 45433.

17. DISTRIBUTION STATEMENT (of the abstract entered in Block 20, if different from Report)

18. SUPPLEMENTARY NOTES

19. KEY WORDS (Continue on reverse side if necessary and identify by block number)

Transfer Lasers, Intermolecular Vibrational Energy Transfer, Deuterium-Hydrogen Chloride, Electric Discharge Excitation

20. ABSTRACT (Continue on reverse side if necessary and identify by block number)

The objective of this investigation is to develop and demonstrate the technology necessary to design a practical airborne molecular vibration-vibration energy transfer laser operating in the 3 to 5 μm spectral range with an output of 10-100 watts. The deuterium-donor/hydrogen chloride-acceptor system has been selected as the most promising transfer system in the given spectral region. Spectroscopic measurements have been made in flowing HCl vibrationally excited by transfer from deuterium excited in a

DD FORM 1 JAN 73 1473 EDITION OF 1 NOV 65 IS OBSOLETE

Unclassified

SECURITY CLASSIFICATION OF THIS PAGE (When Data Entered)

409 252 LB

self-sustained dc electric discharge. The medium is characterized by a vibrational temperature, which is T_V = 1440-1960°K and rotational temperature, which is T_R = 240-325°K immediately after mixing and transfer. Donor gas excitation determined by Raman scattering in the hydrogen isotope corresponds to T_V = 900-1350°K. Calorimetric measurements of electric discharge heat losses have confirmed the relatively low level of discharge vibrational excitation. Attempts to determine post discharge dissociation have been negative.

FOREWORD

This is the final report on work done by United Technologies Research Center, East Hartford, Connecticut, for the Air Force Avionics Laboratory (DHO), Air Force Systems Command (AFSC), under Contract F33615-75-C-1047, Project 2001-01-35 during the period January 1975 to December 1975. The work was monitored for the Air Force by Mr. O. P. Breaux, AFAL/DHO. The report describes the results of an investigation to demonstrate a vibrational energy transfer laser operating in the 3 to 5 micron wavelength band.

The author wishes to acknowledge the assistance of Mr. R. J. Hall who performed the numerical modeling; Mr. V. Failla who assembled and operated the experiments; and Mr. W. L. Nighan and Dr. C. J. Ultee for helpful discussions.

The authors submitted this report for Air Force review on 3 February 1976.

TABLE OF CONTENTS

LIST OF ILLUSTRATIONS

LIST OF TABLES

SECTION I

SUMMARY

The vibrational energy transfer (VET) lasers have been known for over ten years. In this class of device, pumping is based upon the excitation of the vibrational energy levels of one molecular species, typically a diatomic gas, and the rapid exchange of those vibrational quanta to a second selected molecular species, typically a known laser emitter, by near resonant energy transfer. This technique has only recently received attention for applications in the mid-infrared, which would fulfill an important Air Force/DoD requirement.

Computer modeling of these systems, conducted at the United Technologies Research Center, using reliable physiochemical data and an accepted analysis of electron/molecular and molecule/molecule interactions, has indicated that a cw electric discharge excited vibrational energy transfer mixing laser can be an efficient source for continuous laser radiation in the desired 4.0 to 5.0 μm emission band.

Experiments have been conducted on a laboratory VET laser device utilizing the D_2*/HCl system which has been identified as having the most promising potential in the mid-infrared. In these tests, spontaneous emission from transfer excited HCl has been observed and is reported herein. The degree of excitation in HCl has been deduced from these measurements. In addition the degree of vibrational excitation within hydrogen issuing from a dc discharge has been directly measured by Raman scattering. These measurements indicate that first three vibration levels of HCl excited, in this manner, are characterized by a vibrational temperature, T_v = 1400 - 1960°K. The post discharge D_2 vibrational temperature implied by these determinations indicated T_{v_0} = 1300 - 1700°K. The Raman scattering measurements indicated T_v = 900 - 1300°K characterizing the state of hydrogen downstream of a similar discharge. Vibrational relaxation has been measured in these experiments and is much higher than anticipated.

The relatively low discharge efficiencies suggested by these measurements have been confirmed by calorimetric heat balance measurements made on water cooled discharges. The exact explanation of the low discharge efficiency has yet to be determined. Titration experiments using nitrosyl chlorides to measure post discharge atom concentrations indicate concentration levels below the sensitivity of the experiment, as predicted by theoretical calculations. Therefore, it is concluded that H-atom deactivation of the donor gas species is not of sufficient magnitude to account solely for the low degree of excitation observed.

SECTION II

INTRODUCTION

Objective

For certain important Air Force and DoD missions, an efficient low to medium power (10 to 100 watt) source of infrared laser radiation is required. Of particular interest is the 4.0 to 5.0 μm region of the spectrum, corresponding to an atmospheric transmission window. One of the more promising classes of devices to satisfy this requirement is the cw vibrational energy transfer (VET) laser. The objective of the research reported here is to develop the technology base sufficiently to demonstrate the technical feasibility of the VET laser and determine the potential performance characteristics of such devices for airborne use.

The Vibrational Energy Transfer Laser

The VET laser operates essentially in two sequential steps: (1) a donor gas, preferably a diatomic molecule, is vibrationally excited in a separate excitation zone. (2) A second gas, the lasing species, is intermixed with the donor gas, resulting in the transfer of vibrational quanta from the excited donor to the laser species. With carefully matched donor/acceptor molecule pairs and carefully chosen operating conditions, laser emission from the acceptor species can be sustained continuously and efficiently via this pumping route.

There are several distinct advantages of the VET laser concept. The region of vibrational excitation can be separated physically from the region of laser action. Thus different conditions can be established in each of these different regions, affording independent optimization of the excitation step and the transfer and lasing step. A laser species, which either could interfere with or could be decomposed in the excitation process, can be removed from the excitation zone of the VET laser. Therefore, a much greater range of choice of laser species, and hence, a much greater choice of laser emission wavelengths, is created. With a single donor molecule, the laser emission frequency can be tuned by selection of different acceptor species, any of which could be pumped by the single donor molecules. Certain donor molecules which can be excited efficiently, but do not emit in the IR (homonuclear diatomics) can be utilized very effectively in the VET laser device. Vibrational quanta are transferred from the donor species, which do not exhibit optical gain, to an acceptor molecule which can exhibit optical gain (examples

include heteronuclear diatomics, triatomics). If the vibrational energy levels of the donor and laser species are closely matched, the transfer of vibrational quanta between these two species can be very fast and very efficient. Such near-resonant vibrational energy transfer has formed the basis for the pumping of the well-known N_2-CO_2 laser.

Based on previous calculations (Ref. 1) a dc electric discharge appears to be the most promising excitation source. Within an optimized glow discharge, electrical energy can be coupled very efficiently into the vibrational modes of diatomic gases, and thus allows for the study of many different promising donor gases. This rather broad range of study is reported herein. Because the transfer and lasing zones are physically separate from the electric excitation in the proposed VET laser device, a similarly broad range of laser species can be explored.

Calculations indicate that the use of donor (starred)/emitter pairs such as D_2*-HBr and D_2*-HCl in the cw electric discharge VET laser can yield small-signal gain coefficients >1.0 percent/cm and specific laser output powers $\approx$ 50 kJ/lbm on a series of vibrational-rotational transitions of the hydrogen halide molecules distributed through the 4.0 - 5.0 μm region. These same computer calculations (Ref. 1) have identified the little recognized sensitivity of the VET laser medium to poisoning by small concentrations of free atoms. Concentrations of free atoms (e.g., H, F, Cl) as low as 1.0 mol-percent are expected to deplete optical gain in the VET laser medium completely via the extremely rapid relaxation of the vibrationally excited laser emitter, envisioned to be a hydrogen halide. This very rapid vibrational energy decay induced by atom collisions with the emitter completely dominates over vibrational energy transfer pumping of the emitter. Fortunately, continuous self-sustained dc glow discharges can be maintained in selected diatomic gases (e.g., H_2, D_2) with negligible free atom production.

The experimental apparatus and approach chosen for the current investigation, is designed to elucidate the vibrational energy transfer mechanisms, the efficiency of donor excitation and the degree of excitation in the laser gas. The experiment thus has been designed to yield maximum scientific information. The final airborne version of the VET laser, however, may be considerably different. The electric discharge VET laser may be adaptable to premixed, closed-cycle operation. Efficient, light-weight electrical power supplies matched to the power requirements envisioned for the device are available and could be easily integrated into the airborne design. A fully developed electrically-pumped VET laser could be envisioned to operate in a closed-cycle, thereby obviating storage and supply problems. In this mode of operation, an initial charge of donor and acceptor gases would be pumped continuously through a closed loop provided with the necessary discharge and cooling section. Such a system shows great promise for airborne applications.

SECTION III

EXPERIMENTAL INVESTIGATION

The United Technologies Research Center for the past year has investigated the VET laser concept as applied specifically to the D_2*/HCl system. This investigation has had as an objective the study of the characteristics of an actual device. The motivation for the approach is that by characterizing the conditions pertaining in an actual device, (1) an assessment can be made of the appropriateness of theoretical models of the VET laser system which have been developed, (2) the laser potential can be predicted, and (3) a practical knowledge can be obtained about some of the major technology problem areas (at least those which are common to an airborne and a laboratory environment) which must be overcome before the concept can be reduced to practice. The primary diagnostic tool utilized in this study has been the observation of spontaneous emission from vibrationally excited laser species formed as a result of mixing with the discharge excited species. In addition, direct measurements have been made of the vibrational excitation within the donor species downstream of a self sustained dc discharge. This experiment will be described in this section.

Electric Discharge Tubes for Donor Gas Excitation

The self sustained electric discharges used in this study were of a simple design. The discharge tubes are 15 cm long with a 2.54 cm ID. The central portion, 10 cm in extent, is cooled by means of a coolant circulation through a concentric jacket. The coolant is either water or liquid nitrogen. Electrode geometry used in the majority of experiments in this study consisted of an upstream electrode, which was a 0.6 cm tube with slightly flared end, and a downstream electrode (cooled) which was a disc penetrated by a 2.0 cm hole, with rounded edges. The donor gas entered the discharge through the tube of the upstream electrode, the outside of which was insulated, and excited through the hole in the downstream electrode. Under most conditions the flow was sonic or near-sonic at the exit of this tube. The transit time through the discharge was approximately 3 milliseconds. The discharge circuit was ballasted (20 kΩ) to provide stability.

The discharges were operated in the range of p = 10 - 20 Torr, with discharge currents from 30 to 150 mA through each tube. The typical Townsend parameter electric field strength-to-gas number density, was $E/n = 2.0 \times 10^{6} - 2.5 \times 10^{16}$ V-cm^2. At low pressure the presence of striations in these blue discharges was pronounced. Striations were not apparent to the eye at pressures typical of actual operating conditions. No signs of arcing were observed,

however, the liquid nitrogen cooled discharge tube appeared to have a central core of more intense visible emission.

Measurement of Vibrational Temperature by Raman Scattering

Direct measurement of the vibrational excitation of the most interesting donor species by infrared emission techniques is precluded by the lack of a dipole transition moment of the homonuclear donor species. Of course, this same fact insures that vibrational energy once established decays relatively slowly. Vibrational excitation of homonuclear species can be measured by Raman scattering because the occurrence of the Raman spectrum depends on the molecular polarizability and not on the presence of a permanent dipole moment.

In the Raman effect a photon incident on a gas molecule is inelastically scattered. The scattering process can be thought of as an absorption and simultaneous reemission from a virtual state. Stokes shifted emission is observed when the incident photon excites the molecules to a higher vibrational state. The scattered photon energy is less than the incident photon energy by the vibrational quantum energy and hence the outgoing light is down- or red-shifted. The opposite process whereby the photon gains an amount of energy corresponding to the vibrational quantum energy is called anti-Stokes scattering. For anti-Stokes scattering to occur the molecule must be in a vibrationally excited state. Under usual thermal conditions the anti-Stokes component is not observed because the degree of vibrational excitation is low for most gas at temperatures less than 1000°K. However, under discharge conditions where the electrons are coupled more effectively to the vibrational modes than to the translational modes, the vibrational temperature can substantially exceed the translational temperature and the anti-Stokes component can be comparable or larger than the Stokes component. It can be shown that the ratio of anti-Stokes to Stokes scattered intensities, I_{as} and I_s respectively is given by

$$\frac{I_{as}}{I_s} = \left(\frac{\nu_o + \nu_v}{\nu_o - \nu_v}\right)^4 \frac{N_{v=1}}{N_{v=0}} = \left(\frac{\nu_o + \nu_v}{\nu_o - \nu_v}\right)^4 \exp\left[-\frac{hc\nu_v}{kT_v}\right]$$

where ν_o is the incident photon frequency (wavenumber) and ν_v is the vibrational frequency (wavenumber) and $N(v=1)$ and $N(v=0)$ are the populations of the first vibrationally excited state and the ground vibrational state respectively. Thus, the degree of vibrational excitation induced by an electric discharge can be determined by measuring the ratio of anti-Stokes and Stokes scattered light intensities.

Description of the Raman Apparatus

In principal it would be possible to determine the degree of vibrational excitation of the donor species (and the acceptor species as well) directly in the transfer apparatus. However, because of the anticipated difficulties of doing the measurements it was decided to conduct the Raman scattering tests in a separate apparatus where collection efficiency and stray light rejection could be optimized. Figure 1 is a schematic diagram of the laser Raman scattering apparatus. The beam from a Spectra Physics (Model 166) argon-ion laser was brought to a focus in the center of the scattering cell by lens L_1. The divergent beam emerging from the cell was absorbed in a beam dump composed of two colored glass filters set at Brewster's angle to the incident beam and inside a blackened box. Light from the focal volume of L_1 was collected at 90 degrees to the incident laser beam by an achromatic lens, L_2 (f/1.7). Lens L_2 collimated the light and transmitted it to lens L_3 being turned through ~90 degrees at a plane first surface mirror M_3 which was used to facilitate alignment. Lens L_3 refocussed the image of the focal volume onto the entrance slit of a Jarrell-Ash (model 150) 1-m monochromator and was chosen to match the solid angle of the monochromator entrance. The actual orientation of the laser beam was vertical so that the vertical image of the focal volume matched the vertical slit of the monochromator. A spherical front surface mirror M_2 collected back scattered light and focused it at the focal volume and into L_2.

The scattering cell consisted of a rectangular parallelopiped of black anodized aluminum. Three mutually perpendicular holes were drilled through the center of the cell. The laser beam entered through a window perpendicular to the cell. The bore of this hole was threaded to reduce scattered light. The windows were sealed with thick O-rings which allowed adjustment of the windows to achieve parallelism and thereby minimize excess laser beam scattering by multiple reflection and beam walk-off. The second hole allowed collection of scattered light. Discharged gases flowed through the focal volume along the third hole. The surfaces of these holes were sand blasted before the cell was anodized to minimize reflections.

The detector system consisted of a EMI 6256S photomultiplier tube in a Products for Research (Model TE-114B) LN_2 cooled housing at the exit slit of the monochromator. A lens imaged the exit slit onto the PMT cathode. A SSR Instrument photon counter (Model 1140) and discriminator were employed to process the signal.

The discharge used in the tests was identical in form to the discharge used in the transfer apparatus. The only difference between the Raman discharges and the transfer discharge was that the Raman discharge tube and cathode were water cooled instead of LN_2 cooled. A Rayleigh horn was employed

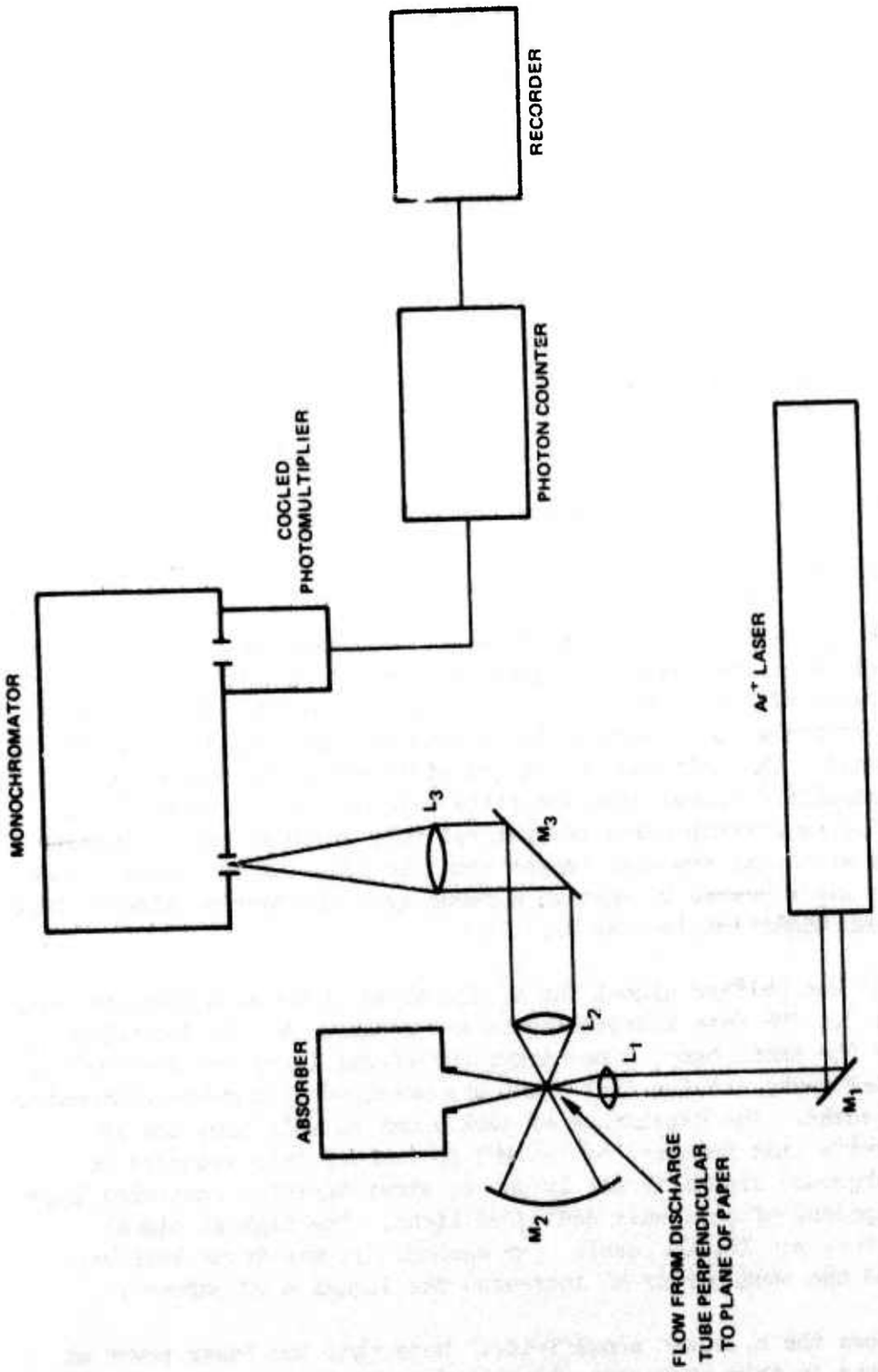

Figure 1. Experimental Arrangement for Raman Measurements

R10--5--1

in a bend in the glassware joining the discharge tube to the scattering cell. The distance between the cathode exit and the laser focal volume was ~ 19 cm.

The overall system spectral response of the Raman system is shown in Fig. 2. Response was measured with a tungsten-quartz-iodine lamp operated at 2400°K as determined by an optical pyrometer. The photon counting rate as a function of wavelength was normalized by the blackbody function (Ref. 2) at 2400°K corrected for dependence of emissivity on temperature and wavelength (Ref. 3). The shape of this curve is determined mainly by the photomultiplier response. The Raman scattered light is polarized, in the present case perpendicular to the grating grooves. The effect of a polaroid filter on the response at the Raman wavelengths was determined and is also shown on Fig. 2 along with transmission of a filter used for some measurements. The curve gives the response to natural light.

The monochromator counter was calibrated with a Hg lamp.

Experimental Results

In order to optimize the system performance, measurements of the Raman Stokes band of nitrogen were made at higher than normal discharge pressures. Usually the entrance slit and exit slit width were set equal. The entrance slit width was determined by observing the effect of narrowing the slit width on the Raman signal. The slit was set at the width which just began to decrease the transmitted signal when the slits were narrowed. Normally the slit width was 0.6 mm corresponding to spectral full width at half intensity of 0.5 nm. This width was somewhat larger than the image of the focal volume would be for the laser beamed brought to a focus by a diffraction limited lens (collection system magnification was 4.5).

The Raman Stokes shifted signal for N_2 signal is shown as a function cell pressure in Fig. 3. The data labeled Stokes are measured at the intensity peak on scanning the Raman band. The background signal level was recorded 0.6 nm from the signal peak, and the dark count was measured with the monochromator entrance slit blocked. The dependence of dark count on cell pressure is attributed to finite time required by the PMT to recover from exposure to lights. The background signal is mainly due to stray Rayleigh scattered light with a small component of cell wall scattered light. The highest signal recorded at 760 Torr was 16,000 counts per second. It was found that when properly adjusted the back mirror M_2 increased the signal ~ 60 percent.

Figure 4 shows the hydrogen sensitivity. Note that the laser power at 488 nm is 1.4 watts in this case compared to 1.0 watts for the nitrogen data shown in Fig. 3. The lower overall sensitivity to hydrogen is mainly attributable to lower photomultiplier response at the longer H_2 wavelength (the

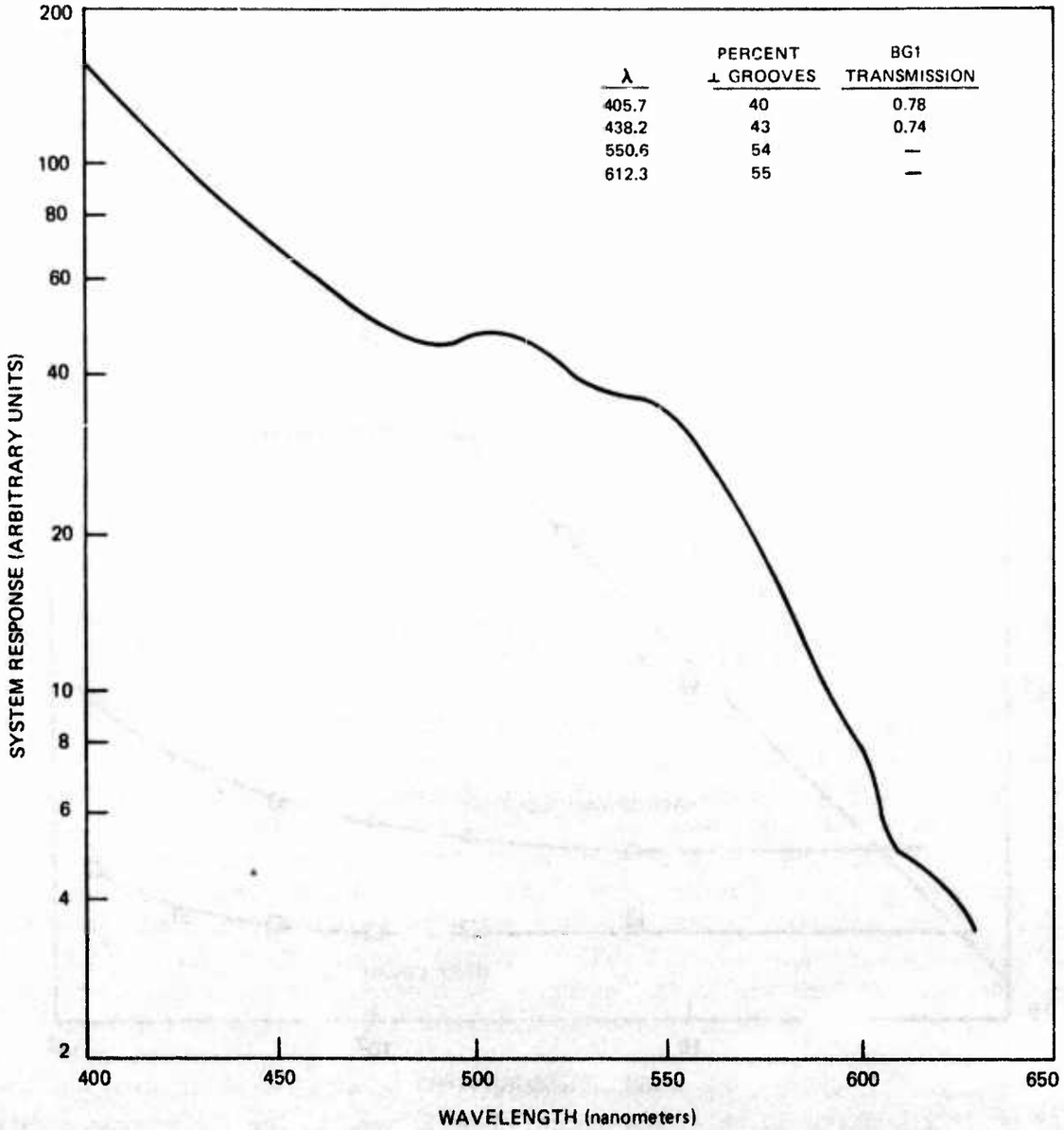

Figure 2. Raman System Spectral Response

R10-5-2

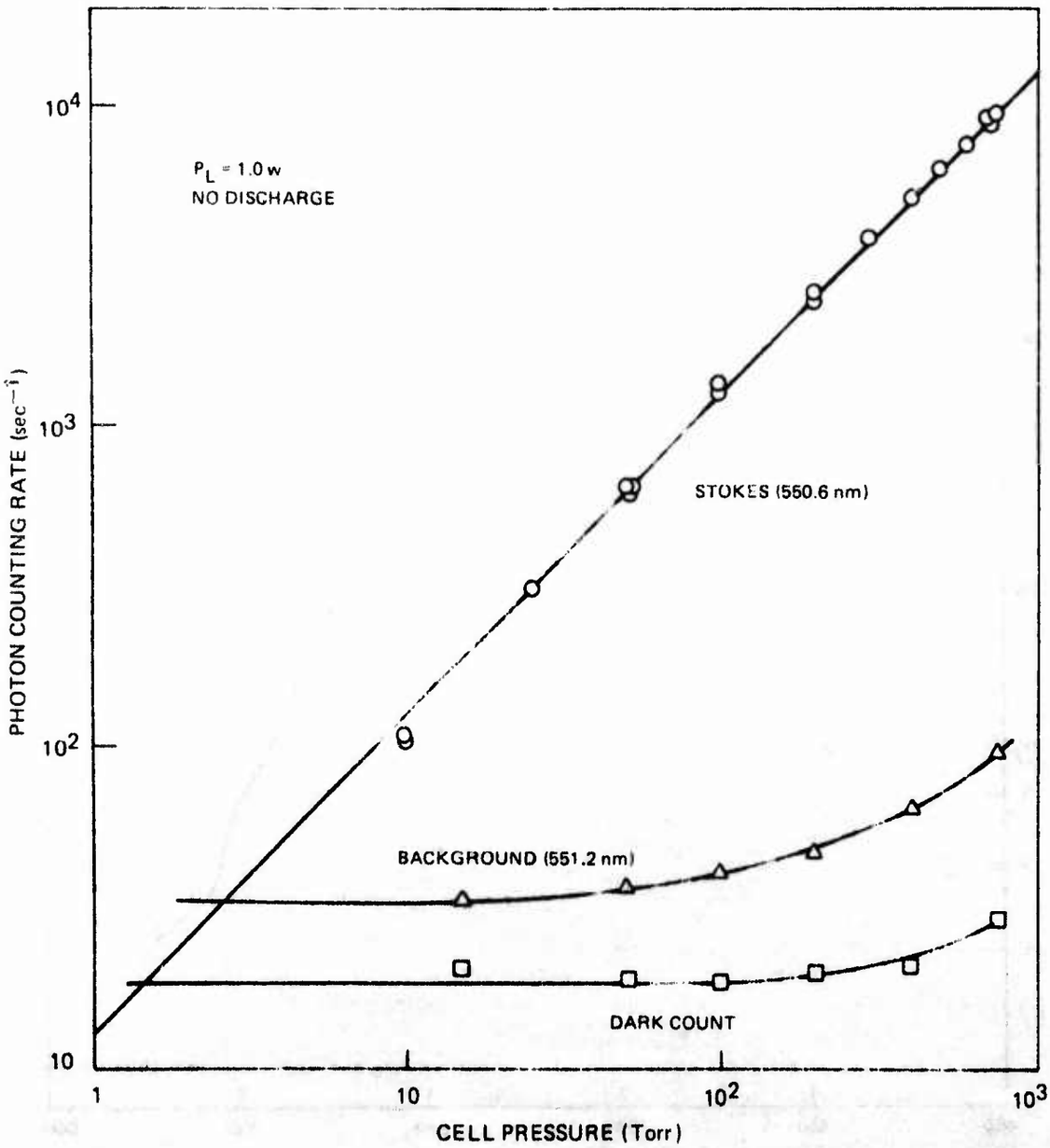

Figure 3. Nitrogen Stokes Sensitivity

R10-5-4

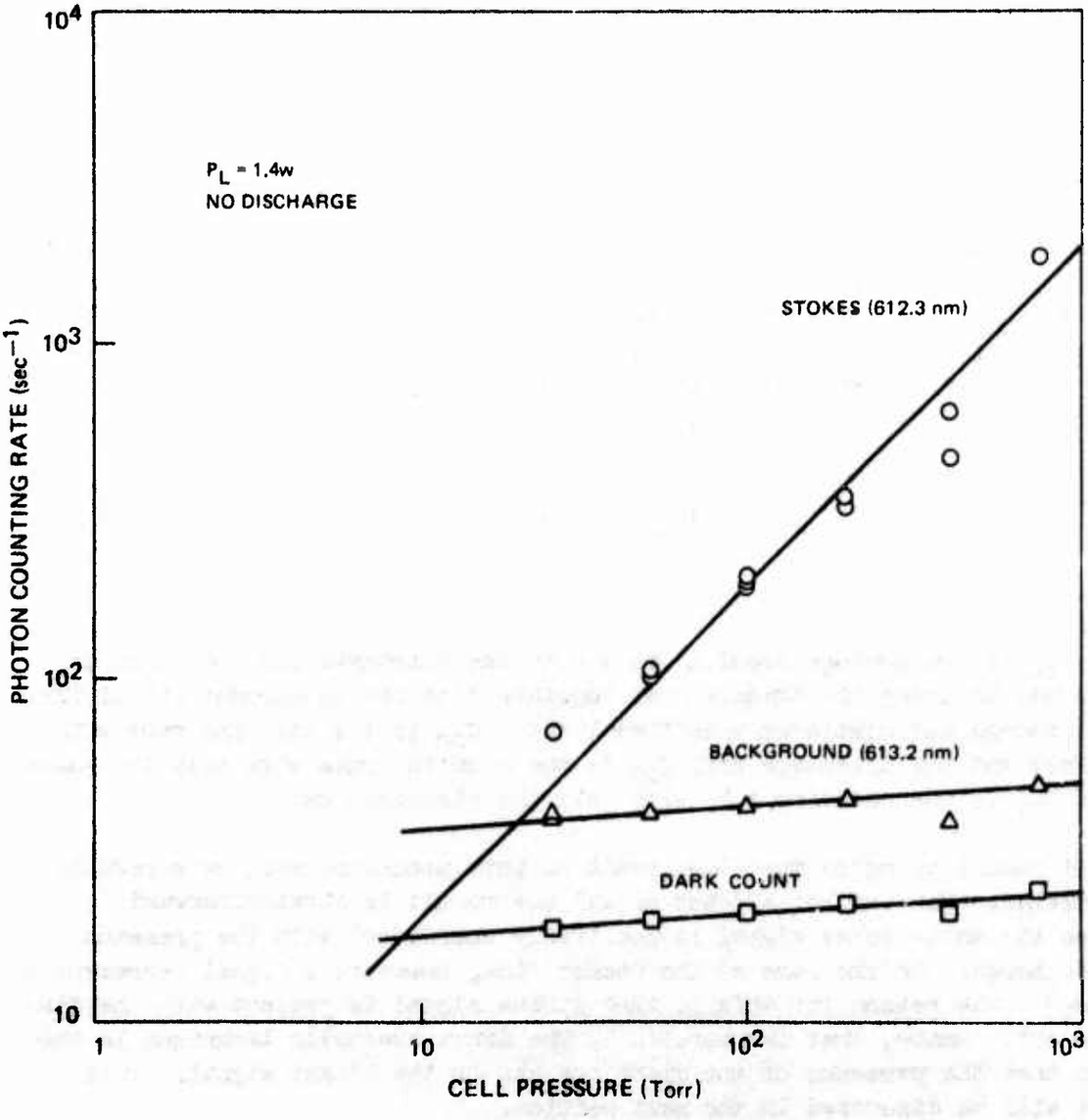

Figure 4. Hydrogen Stokes Sensitivity

R10-5-3

hydrogen Raman cross section is approximately twice the nitrogen cross section, Ref. 4). The fact that the background signal is less dependent on cell pressure probably reflects the lower Rayleigh scattering coefficient in hydrogen (Ref. 5).

When measurements of anti-Stokes signals were attempted under discharge conditions several problems arose. The first problem to manifest itself in nitrogen was the presence of a Lyman grating ghost at a wavelength equal to 0.9 of the parent 488 nm argon ion line. This places the ghost ~1 nm from the N_2 anti-Stokes line. This line actually presents no problems to the measurement of the anti-Stokes signal (it can be discriminated against by a Schott BG-1 filter) except on scanning it can be mistaken for the Raman signal. The second problem arose because of the large background signal levels present in the afterglow. Background and anti-Stokes signal levels were such that the anti-Stokes signal was not apparent on scanning the monochromator across the spectral region of the band. For the anti-Stokes measurements the monochromator was set at the Raman anti-Stokes wavelength and a signal averaging technique was employed. This techniques has been employed previously to minimize background effects in $N_2(v)$ measurements (Ref. 6). The Raman signal is determined from four consecutive counting periods during which the counting rate is averaged on a chart recorder. The Raman signal is obtained from

$$C = C_{11} + C_{00} - C_{10} - C_{01},$$

where C_{11} is the average counting rate with the discharge and the laser on (and hence includes the Raman signal together with the background signal from the discharge and scattered unshifted light), C_{00} is the counting rate with the laser and the discharge off, C_{10} is the counting rate with only the laser on and C_{01} is the counting rate with only the discharge on.

It should be noted that the result of this procedure must be carefully interpreted. For the anti-Stokes signal the result is straightforward because the anti-Stokes signal is positively correlated with the presence of the discharge. In the case of the Stokes line, however, a signal decrement is measured. The reason for this is that Stokes signal is present with the discharge off. Hence, what is measured by the above averaging technique is the effect that the presence of the discharge has on the Stokes signal. This effect will be discussed in the next section.

The Effect of Vibrational and Gas Temperatures on Stokes Scattered Intensities

Equation (1) gives the ratio of anti-Stokes signal to the Stokes signal when the afterglow region is characterized by a vibrational temperature T_v and a gas temperature T. This equation cannot be applied directly to data in which the Stokes signal has been measured with the discharge off. The data in Figs. 3 and 4 must be corrected for the effect of T_v and T before being used.

When a molecule in a state characterized by vibrational and rotational quantum numbers v and J respectively undergoes a transition in a state v', J' the intensity of Raman scattered light can be shown (Ref. 7) to be

$$I^{v,J}_{v',J'} \sim n \frac{g_I(2J+1)(v+1)}{Q_v(T_v)Q_R(T_R)} \; b^J_{J'} \; \exp\left[-\frac{E(v,0)}{kT_v} - \frac{hcB_oJ(J+1)}{kT}\right] \qquad (2)$$

where n is the gas number density and g_I is nuclear spin degeneracy, Q_v and Q_R are the vibrational and rotational contributions to the partition function, $b^J_{J'}$ is the Placzek-Teller coefficient (Ref. 7), E(v,0) is the energy of the v-th vibrational level for J = 0, B_o is the rotational constant of the ground vibrational state and the remaining physical constants have their usual meanings. Those parts of this relationship which depend on the gas density and molecular parameters can be factored out to define the relative line intensity $S^{v,J}_{v',J'}$;

$$S^{v,J}_{v',J'} \equiv \frac{g_I(2J+1)}{TQ_R(T_R)} \; b^J_{J'} \; \exp\left[-hcB_oJ(J+1)/kT\right] \qquad (3)$$

Now the rotational partition function can be approximated in the temperature range of interest by

$$Q_R \approx \frac{(2I+1)^2kT}{2hcB_o}$$

where I is the nuclear spin. So that equation (3) can be written

$$S^{v,J}_{v',J'} = \frac{g_I(2J+1)\theta_R}{(2I+1)^2T^2} \; b^J_{J'} \; \exp\left[-\frac{J(J+1)\theta_R}{T}\right] \qquad (4)$$

where $\theta_R = hcB_o/k$ is the characteristic rotational temperature. Restricting discussion to the vibrational Q branch ($J' = J$) which is most intense the Placzek-Teller coefficient can be written (Ref. 7)

$$b^J_{J'} = \frac{J(J+1)}{(2J-1)(2J+3)} + a_o \qquad \text{(Q-branch)} \qquad (5)$$

where $a_o = (3-4\rho_p)/4\rho_p$ is the trace scattering coefficient and ρ_p is the depolarization ratio for polarized light.

The effect of gas temperature on the relative Q-branch intensities can be interpreted in a straightforward manner from Equation (4). The T^{-2} dependence arises from the combined effect of gas density and rotational partition function. The exponential gives the effect of temperature on the individual rotational lines. The Q-branch transitions in nitrogen are more closely spaced in wavelength than for hydrogen because of the higher moment of inertia. In fact, all the lines of N_2 Q-branch fall within the bandpass of the monochromator. Summing over all lines, the rotational partition function is recovered, so that for N_2 $\sum_J S^{oJ} \sim T^{-1}$. For hydrogen the various Q branch transitions are separated enough that some lines fall outside of the monochromator bandpass. Thus increasing temperature has the tendency of shifting the peak of the line intensities out of the monochromator bandpass. The locations of the first four H_2 Q-branch transitions have been calculated and are shown in Table 1 for a 488 nm exciting line.

TABLE 1

H_2 Q BRANCH WAVELENGTHS

Transition	Wavelength (nm)
v=0, J=0	612.27
J=1	612.05
J=2	611.60
J=3	610.93

Now for hydrogen $g_I = 3$ for the odd J levels, and $g_I = 1$ for the even levels and the nuclear spin is $I = 1/3$, see Ref. 6. The depolarization ratio has been measured for natural light: $\rho_n = 0.070$-0.073 (Refs. 8 and 9). The depolarization ratio for polarized light is related to the natural light

depolarization by $\rho_p = \rho_n(2-\rho_n)$, so that the trace scattering coefficient is $a_o = 18.7\text{-}19.8$. Here $a_o = 19$ has been used. The relative intensities of several Q branch transitions have been calculated as a function of gas temperature and are shown in Fig. 5. Because of the variation of nuclear degeneracy and the exponential, the S^{01} intensity is dominant. A simple sum of all five transitions has a $T^{-1.55}$ dependence.

Now the Stokes signal under discharge conditions, $C_s(T_D, T_v)$ can be related to the Stokes signal with the discharge off, $C_s(T_o)$:

$$C_s(D) = \frac{C_s(0)f(T)}{Q_v(T_v)}$$

where

$$f(T) = \frac{T_o}{T_D} \text{ for } N_2$$

and

$$f(T) = \left(\frac{T_o}{T_D}\right)^{1.55} \text{for } H_2$$

and use has been made of the fact that $Q_v(T_v = T_o) = 1.0$. T_o is the initial gas temperature and T_D is the post discharge temperature. Equation (1) can now be written

$$Q_v(T_v) \exp \frac{\theta v}{T_v} = \frac{C_s(T_o)f(T)}{C_{as}(T_D)} \frac{R_{as}}{R_s} \left(\frac{\nu_o+\nu_v}{\nu_o-\nu_v}\right)^4 \qquad (6)$$

where R_{as} and R_s are the system responsivity at the anti-Stokes and Stokes wavelengths, respectively (see Fig. 2).

The post discharge vibrational temperature can be calculated from Equation (6) using the gas temperature factor f(T), or directly from discharge measurements of both Stokes and anti-Stokes. Both of these procedures have been used. It was found that, in nitrogen that the signal averaging procedure resulted in taking the differences (small) of large numbers, due to the presence of a large background signal when the BG1 filter wasn't used. This led to a large experimental uncertainty so that except for one measurement in which the BG1 filter was used, the nitrogen data has been reduced using Equation (6) along with a post discharge gas temperature calculated from known heating rates. The background signals in the case of H_2 weren't large and the results of using Equation (6) with extrapolated discharge off data and using discharge data directly were in good agreement. The results of several experiments are shown in Table 2.

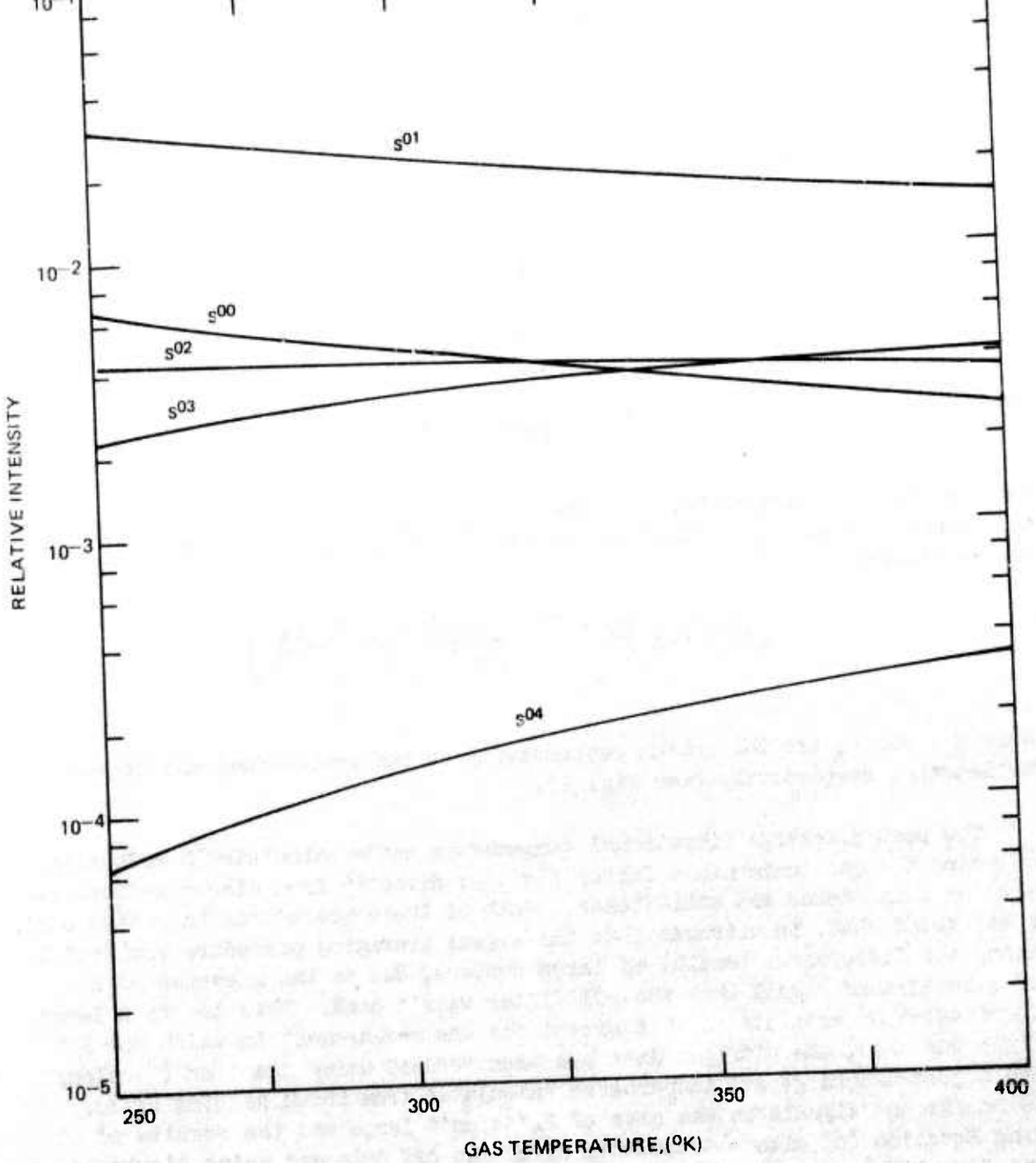

Figure 5. Calculated Stokes Vibrational Q–Branch Intensities for H_2

R10–9–1

TABLE 2

RAMAN VIBRATIONAL TEMPERATURE MEASUREMENTS

Gas	p (Torr)	i_d (mA)	V_d (kV)	C_{as-1} (sec^{-1})	C_{s-1} (sec^{-1})	T_v °K
N_2	10	30	2.50	26	40	1710
	14	30	2.15	42	87*	1360
	14	60	2.00	51	80*	1558
	14	75	1.85	70	78*	2290
H_2	20	30	2.30	4.5	21.5	926
	20	60	2.15	10.5	20	1080
	20	90	2.00	13.5	19	1142
	11.5	30		30	19*	1350
	20	50	3.10	19	36*	1140
	21	30	3.90	41	29	1310+

*data reduced using Equation (6) and Figs. 3 and 4.

+all data except this used the sonic tube anode discharge design. This experiment used a radial injector design discussed in Section IV.

Vibrational Energy Transfer Experiments

The vibrational energy transfer apparatus has been described previously (Ref. 1) so that here only the salient features will be reiterated and modifications made to the previous apparatus will be described. In the transfer apparatus (Fig. 6) gases excited in two 2.54 cm diameter discharge tubes flow through constant area transition sections to two 0.4 cm high, 12.5 cm wide channels. A secondary gas is injected into the main flow through 88-0.010 inch holes drilled in a single row, through the top and bottom, channel walls at the beginning of the parallel wall central section, see Fig. 7. The gases exit through two transition sections to a chemical trap charged with zeolite and hence to a large (nominally 600 cfm) vacuum pump. For safety, nitrogen is added to the flow after the chemical trap. The channels are joined together at the center and the sidewalls are closed by Brewster angle window holders in which CaF_2 windows are used. The windows are purged with an inert gas.

The modifications which have been made to the apparatus include the addition of cooling coils to the outer top and bottom surface of the nickel

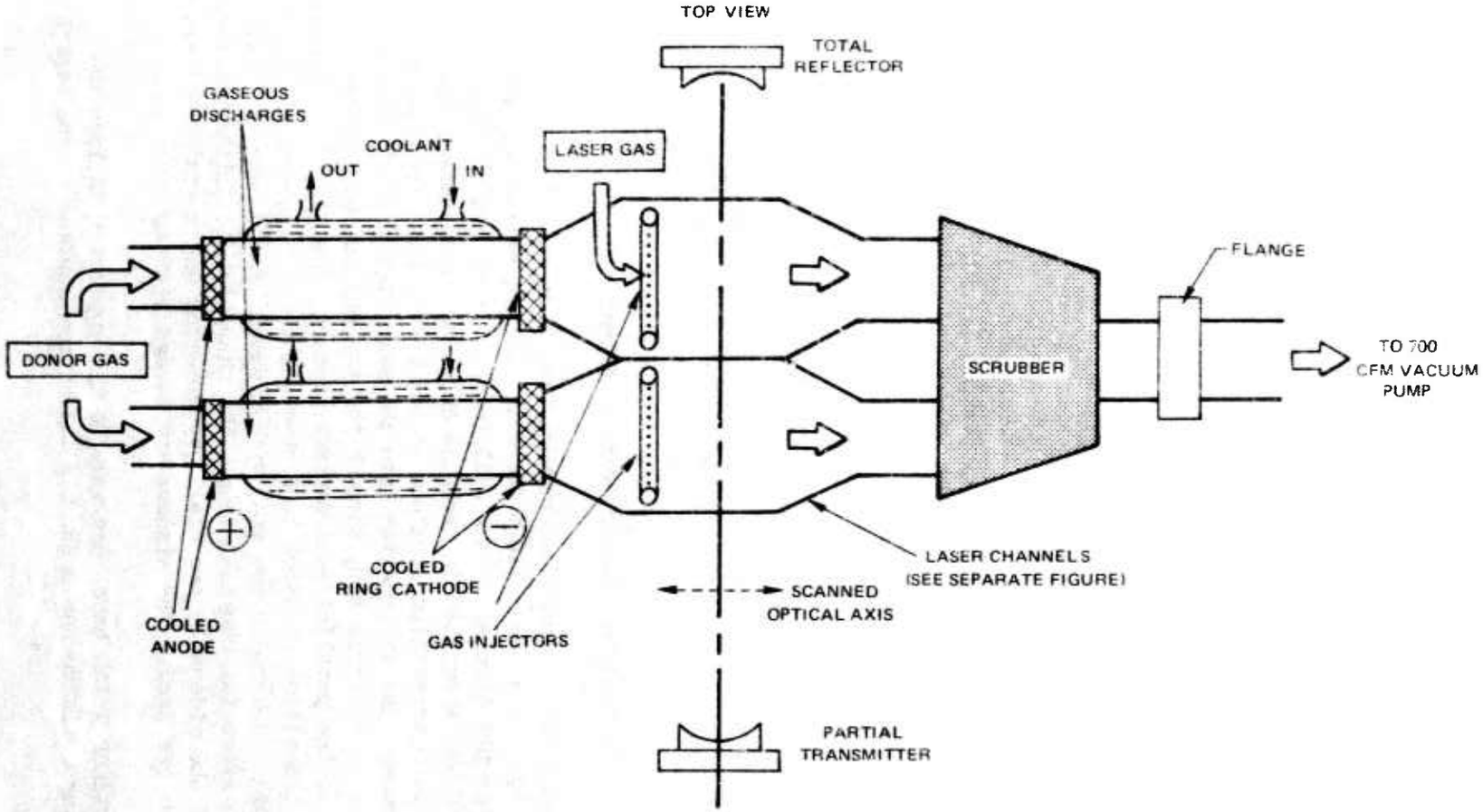

Figure 6. Vibrational Energy Transfer Laser Apparatus

N09-62-1

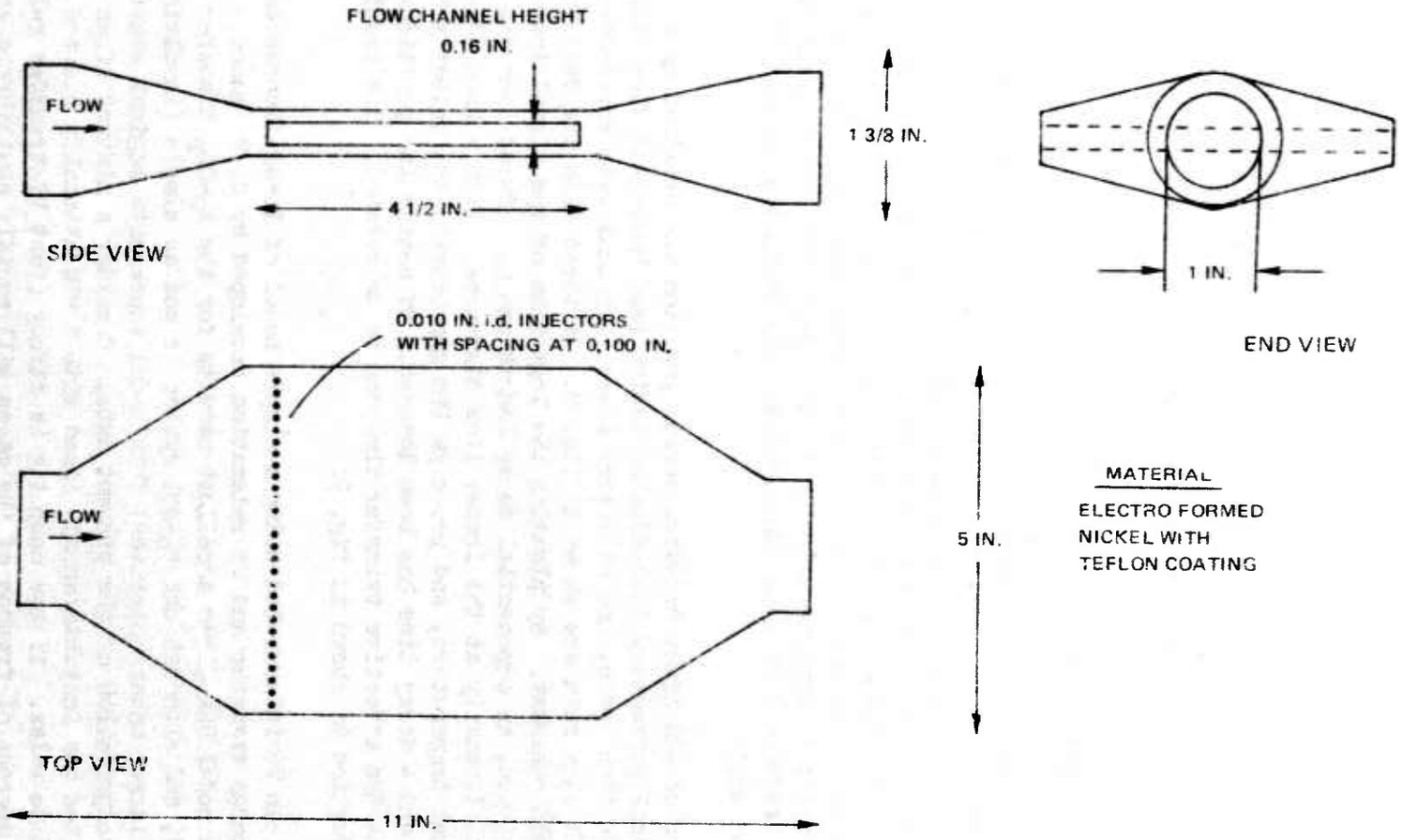

Figure 7. Laser Channel Design

channels. Alcohol is circulated through these coils and through a heat exchanger coil in a dry ice/alcohol mixture by two centrifugal pumps. In another modification the injector manifold has been constructed of copper bar and is bonded to the channels. This manifold is cooled by a loop in the alcohol coolant circuit. Indium has been used to seal the discharge tubes which are LN_2 cooled. With these seals a leak rate corresponding to 0.01 percent of the total flow has been maintained over a period of many thermal cycles of the apparatus.

HCl Band Emission Experiments

Radiation from the HCl vibrational fundamental band has been examined in the transfer apparatus as a function of distance downstream from the sidewall injector. A LN_2 cooled lead sulfide detector with a 3 mm x 10 mm chip was moved parallel to the flow direction on a stable translation stage. A narrow bandpass filter ($3.6 \pm 0.6\ \mu$) in front of the detector isolated the low-lying vibrational transitions of HCl. A tuning fork chopper modulated the sidelight emission signal prior to amplification by a PARC (Model 124) tuned amplifier. A 7 mm diameter aperture 4 cm from the detector chip defined a narrow (5° half angle) collection angle.

The behavior of sidelight emission versus position was examined as a function of several parameters including deuterium (and hydrogen) flow rate, hydrogen chloride flow rate, and discharge power. Typical data representing the effect of HCl flow rate are shown in Fig. 8. In these data the deuterium flow rate was held constant. By plotting the logarithm of the signal intensity against distance, an exponential decay length can be deduced from the falloff in signal intensity at the longer flow distances. With a knowledge of the gas flow rates temperature, and pressure the gas density and velocity has been calculated and a decay time has been deduced. By noting the positions of the signal maxima the effective transfer time can be calculated. The result of this data reduction is shown in Fig. 9.

These data can be interpreted using a simple model of laser fluorescence involving V-V energy transfer and VT relaxation developed by C. B. Moore (Ref. 10). This model has given excellent results for the N_2-CO_2 transfer system (Ref. 11), and although the D_2-HCl system is not as simple (involving more levels and larger anharmonicities) this model represents logical starting point in the interpretation of the present data. Consider a mixture of an initially unexcited gas instantaneously mixed with a vibrationally excited gas which is allowed to relax. If the coupling is strong (fast VV transfer rate) the vibrational degrees of freedom of the gases will rapidly equilibrate and the two species will return together to equilibrium with the surroundings.

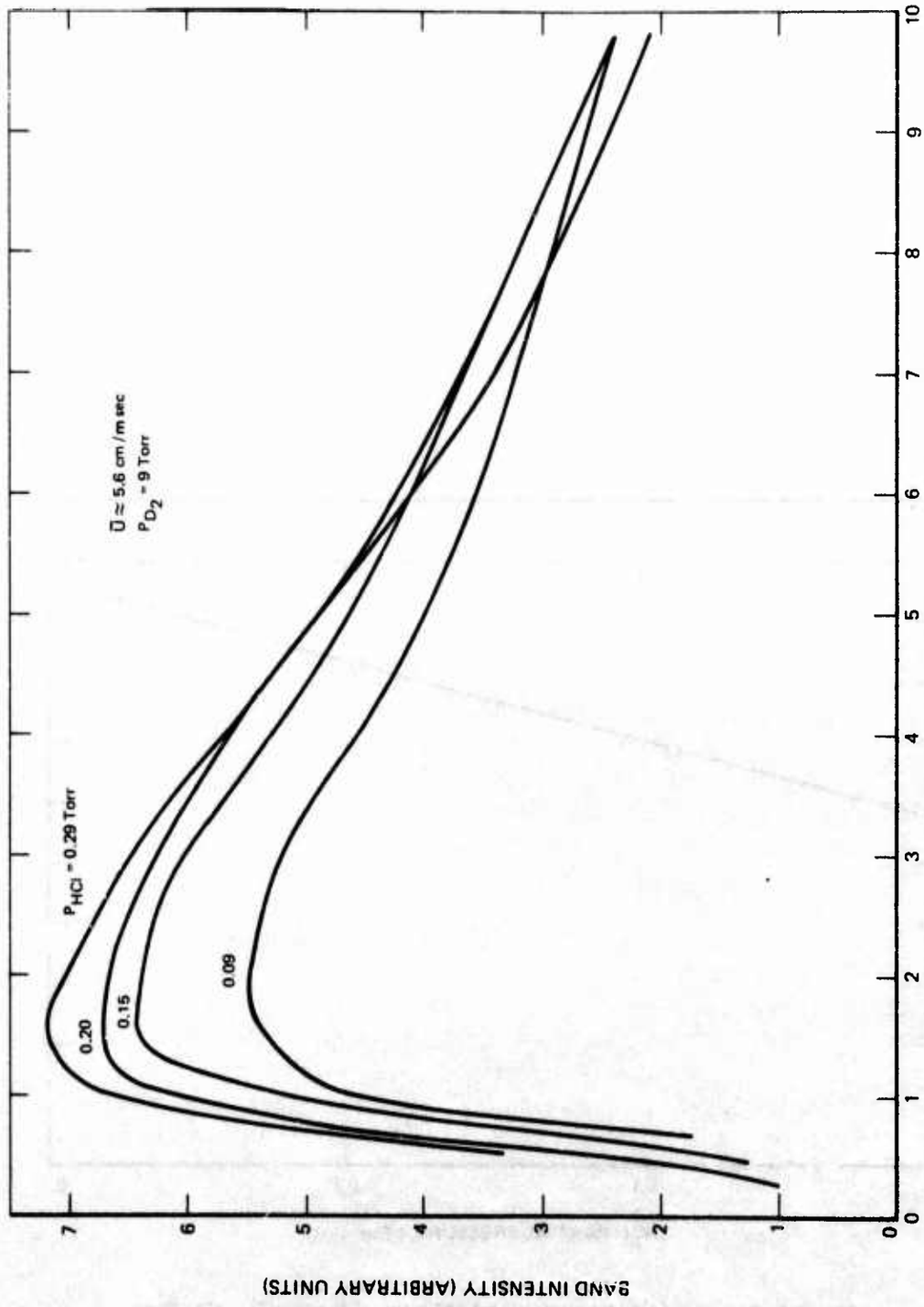

Figure 8. Decay of HCl Band Emission

R10-28-6

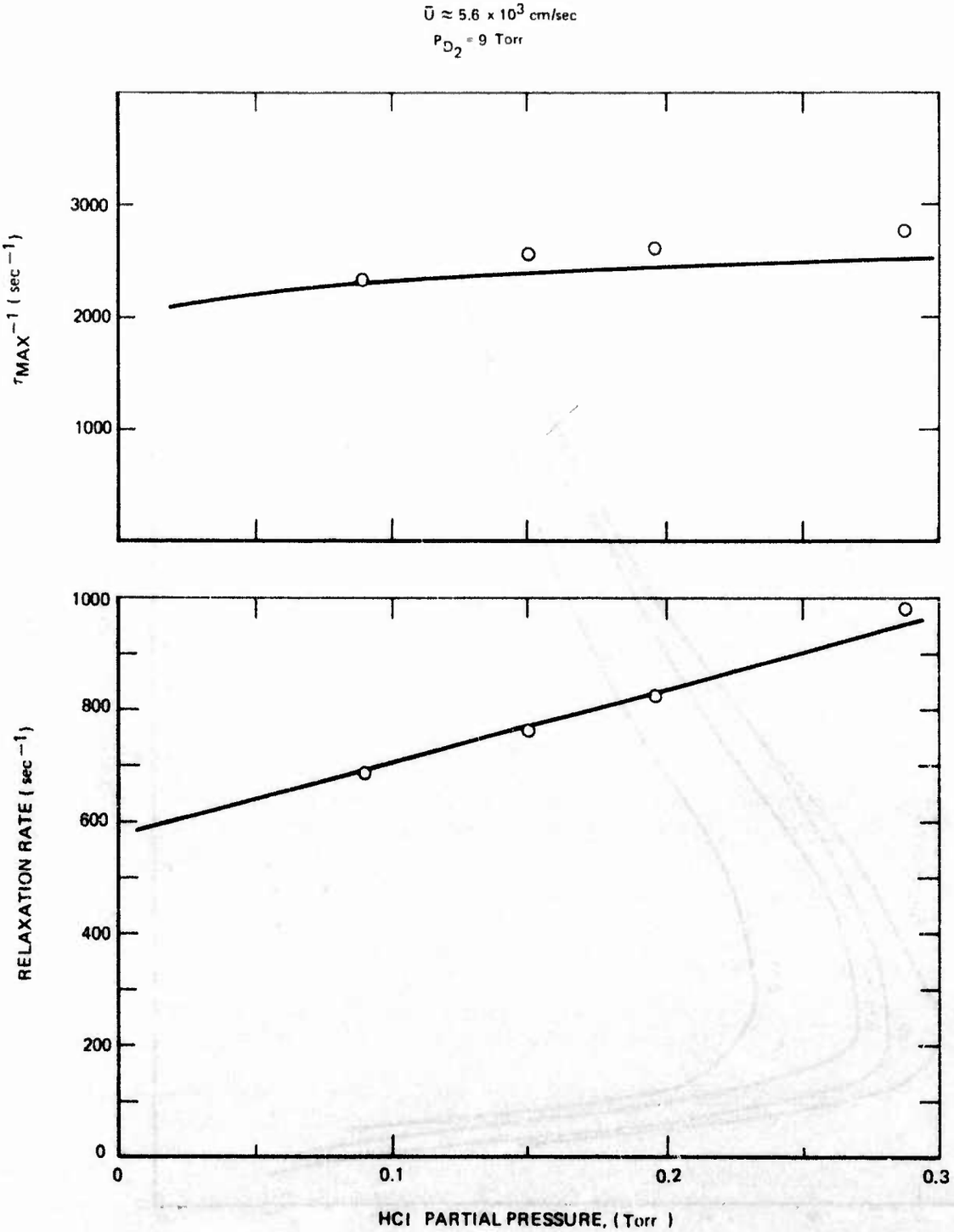

Figure 9. Experimental Relaxation and Vibrational Energy Transfer Data

R10–28–5

The period of mutual equilibration is characterized by the VV transfer time and the period of relaxation is determined by the overall relaxation rate. In Moore's model analysis the individual population densities n_i are given by

$$n_i = A_i e^{\lambda_1 t} + B_i e^{\lambda_2 t} \tag{7}$$

For the initially unexcited gas $A_i = B_i$. The exponentials λ_1 and λ_2 are both negative and are given exactly in Ref. 10. When the VV transfer time is much faster than the relaxation rate then exponential factors are given approximately by

$$-\lambda_1 = k_e[D_2] + k_{e'}[HCl]$$

and

$$-\lambda_2 = \frac{k_{11}[HCl] + [k_{12} + \frac{k_e}{k_{e'}} k_{21}][D_2] + k_{22}k_e[D_2]^2/[HCl]k_{e'}}{1 + \frac{k_e}{k_{e'}} \frac{[D_2]}{[HCl]}} \tag{8}$$

where the rate constants are associated with the following reactions

$$D_2(1) + HCl(0) \underset{ke}{\overset{ke'}{\rightleftharpoons}} D_2(0) + HCl(1) + \Delta E$$

$$HCl(1) + HCl \xrightarrow{k_{11}} HCl(0) + HCl$$

$$HCl(1) + D_2 \xrightarrow{k_{12}} HCl(0) + HCl$$

$$D_2(1) + HCl \xrightarrow{k_{21}} D_2(1) + HCl$$

$$D_2(1) + D_2 \xrightarrow{k_{22}} D_2(0) + D_2$$

The time to the peak HCl density can be found by differentiating Equation (7) and setting the result equal to zero, thus

$$t_m = \frac{1}{\lambda_2 - \lambda_1} \ln \frac{\lambda_1}{\lambda_2} \tag{9}$$

Equation (8) has been solved for rate constant values taken from the literature (Refs. 12-14). The result is shown as the solid line in the upper portion of Fig. 9. Note that it has been necessary to add a constant = 0.3 msec to the data to simulate the effects of mixing. A constant is reasonable because of the nearly constant total pressure. An estimate can be made of the laminar mixing time from

$$t_{mix} \sim \frac{l^2}{4D}$$

where l is the mixing scale (set equal to the distance between injection holes) and D is the binary diffusion coefficient (15). The mixing time is calculated to be 0.6 msec for the present mixer. Thus the mixing time required to produce agreement with the experimental data is not unreasonable.

The rate constant λ_1 is much faster than λ_2 so that considering the behavior of HCl population the exp ($\lambda_1 t$) term rapidly vanishes and the HCl emission decays as exp ($\lambda_2 t$). The lower portion of Fig. 9 can be interpreted as a representation of the experimental variation of $-\lambda_2$ as a function of the hydrogen chloride partial pressure. Comparing the experimental variation of relaxation rate with the rate calculated from Eq. (8) using the individual rate constants calculated by previous investigators (Refs. 12-13) show agreement with the numerator of the λ_2 expression. However, the denominator is large because of the large excess of deuterium over hydrogen chloride. Hence, the overall decay rate is in poor agreement with the decay rate of the simple model.

Spectrally Resolved Sidelight Emission

Emission from the vibration-rotation transitions of HCl was observed at a position approximately 2.0 cm downstream from the injector corresponding very nearly to the location of peak HCl band emission (discussed in the previous paragraphs). The UTRC emission spectroscopy diagnostic system has been described in detail previously (Ref. 16). The system is built around a McPherson 0.3 meter (Model 218) scanning monochromator. Emission is imaged one-to-one onto the entrance slit of this instrument by a 1 m focal length toroidal front surface mirror. Radiation exiting the monochromator is focused by an ellipsoidal mirror onto a InSb (PV) detector. The detector signal is preamplified and introduced into a PARC (Model 124) lock-in amplifier. A 2000 Hz chopper in front of the entrance slit modulates the radiation and provides a reference signal for the phase sensitive amplifier. Normally the entrance slits were 250μ wide (and 6 mm high) corresponding to a resolution of approximately 2 cm^{-1}. The emission apparatus was focused through the CaF_2 channel windows to a point in the center of the channel nearest to the monochromator. The top and bottom channel walls limit the collection aperture. The monochromator system was calibrated by a blackbody source, normally operated at

800°K, set near the apparatus. When a calibration was required an aluminum front surface mirror reflected radiation from the blackbody into the emission apparatus. The response, checked on each run, was relatively flat over the spectral range explored here.

The emission from vibrationally excited hydrogen chloride has been recorded on a strip chart recorder along with a wavelength reference. A typical spectrum is shown in Fig. 10. The vibration-rotation transitions (labeled $P_v(J)$ = v, J-1 → v-1, J and $R_v(J)$ = v, J+1 → v-1, J) of the v = 1 → 0, 2 → 1 and 3 → 2 bands are clearly resolved. The R branch has been resolved but is not shown. The intensities of the v = 3 → 2 transitions are near the detection limit of the monochromator system. The emission signal is uncorrected for the system spectral response. In order to do so the peak signal voltage, V_S, is normalized by

$$I_s = \frac{V_S N_\lambda}{V_{BB}}$$

where V_{BB} is the blackbody voltage response of the system at wavelength λ and $N\lambda$ is the blackbody function, usually expressed in w cm^{-2} μm^{-1} SR^{-1}, and I_s is the reduced signal intensity.

Analysis of Spectral Data

In order to deduce population distributions from the reduced intensities it is necessary to know the radiative transition rates. The intensity of a transition v', J' → v, J is given by

$$I_{v'J',vJ} = A_{vJ}^{v'J'} N_{v'J'} h c \nu_{v'J',vJ} \qquad (10)$$

where $A_{vJ}^{v'J'}$ is the Einstein transition probability (sec^{-1}), $N_{v'J'}$ is the population density of the energy level characterized by quantum numbers v and J (cm^{-3}), and $\nu_{v'J', vJ}$ is the wavenumber of the transition (cm^{-1}). Now if the vibrational mode is characterized by temperature T_v and the rotational modes by T_R the population of level v'J' can be written

$$N_{v'J'} = \frac{N(2J'+1)}{Q_v Q_R} \exp\left[- \frac{G_o(v')hc}{kT_v} - \frac{B_{v'}hcJ'(J'+1)}{kT_R} \right] \qquad (11)$$

where Q_v and Q_R are the vibrational and rotational partition functions respectively, N is the total gas number density, $G_o(v')$ is the energy of v' level with respect to the vibrational ground state (in cm^{-1}), B_v is the

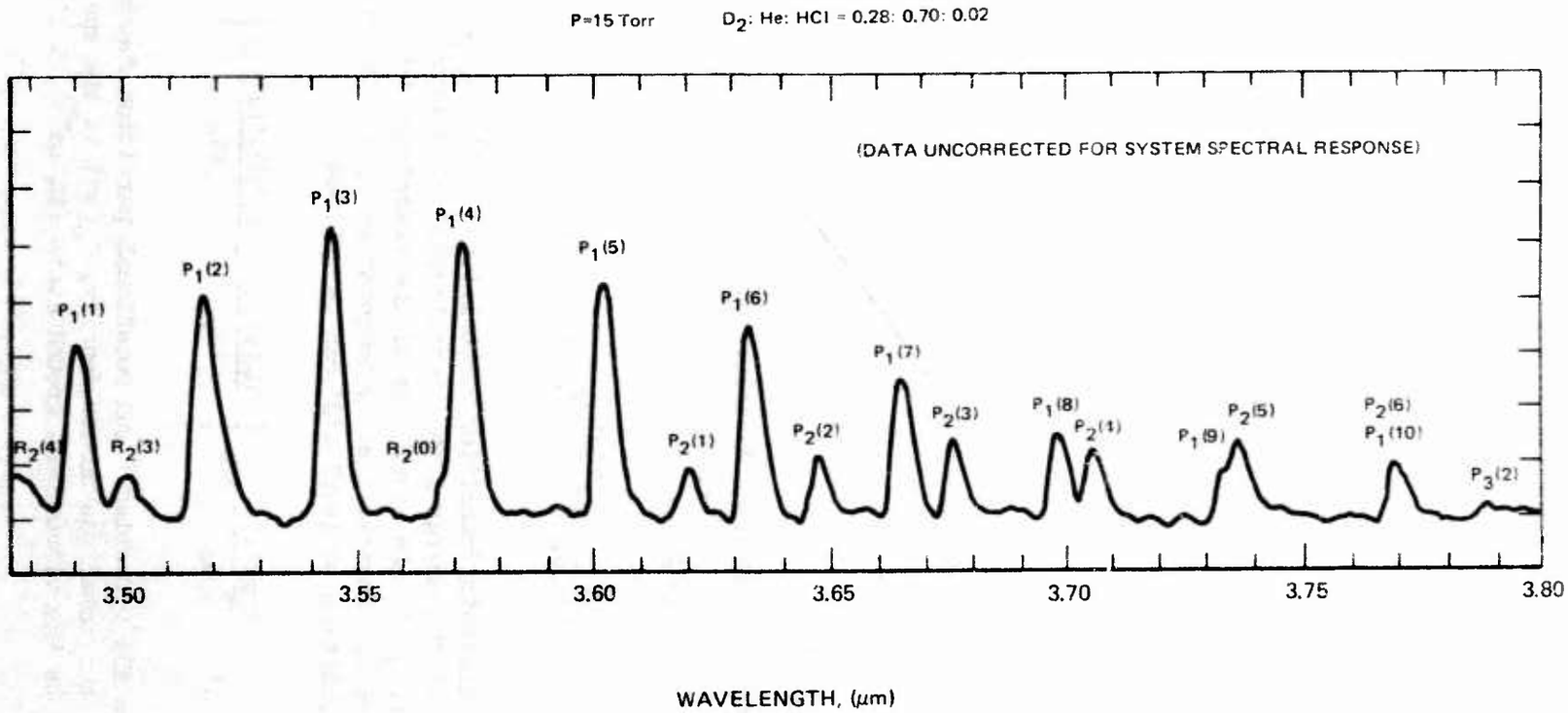

Figure 10. Typical D_2^*–HCl Spontaneous Emission Spectra

rotational energy spacing of the v' level, and (2J'+1) gives the degeneracy of the J' level. The Einstein transition probability can be written

$$A_{vJ}^{v'J'} = \frac{64\pi^4 \nu_{v'J',vJ}^3}{3h} \frac{|R_v^{v'}|^2 F_{vJ}^{v'J'} S_{J'J}}{2J'+1} \qquad (12)$$

where $|R_v^{v'}|^2$ is the pure vibrational dipole transition moment, $F_{vJ}^{v'J'}$ is the vibration-rotation interaction factor and $S_{J'J}$ is the rotational transition moment ($S_{J'J} = J'$ for the R-branch and $S_{J'J} = J'+1$ for the P-branch).

The fundamental band vibrational transition dipole moment is usually taken as proportional to v' (Ref. 17), i.e.,

$$R_{v'-1}^{v'} = v'|R_o'|^2. \qquad (13)$$

The vibration-rotation interaction factor has been measured from absorption spectra (Ref. 18), the result is

$$F(m) = 1 + .026\ m$$

where m = J' for the R-branch and m = -(J'+1) for the P-branch.

By combining these expressions and rearranging it is easy to show that

$$\ln\left(\frac{I_{v'J',vJ}}{\nu_{v'J',vJ}^4 S_{J'J} F_{vJ}^{v'J'} v'}\right) - \ln C = -\frac{B_v hc}{kT_R} J'(J'+1) \qquad (14)$$

where $C = 64\pi^4 c|R_o'|^2 N_v 1/Q_v$. $I/\nu^4 SFv'$ is the normalized intensity. If the analysis is restricted to the P-branch: $J' = J-1 \rightarrow J$, Equation (14) can be written

$$\ln \frac{I_{v'J',vJ}}{\nu_{v'J',vJ}^4 JF_{J'}^{v'}} - \ln C = -\frac{B_v hc}{kT_R} J(J-1)$$

Thus the familiar result, the logarithm of the normalized intensity is proportional to J(J-1) is obtained. The rotational temperature can be obtained by plotting the normalized signal intensities of the various transitions $P_v(J)$

as a function J(J-1). The rotational temperature can be obtained from the slope of the line fitted to the experimental data. The vibrational population densities are proportional to the intercept of the fitted lines with the axis. The vibrational temperature can then be deduced from

$$\ln N_v \sim \frac{I}{\nu^4_{JFv'}}\Bigg|_{\text{intercept}} \sim \frac{G_o(v')hc}{kT_v}$$

A typical rotational distribution plot is illustrated in Fig. 11. The rotational temperature from these data is $T_R = 325^oK$. Note that some transitions are missing, specifically $P_1(9)$ and $P_2(6)$, because they overlap each other and are totally unresolved. The scatter of the $3 \rightarrow 2$ data is typical and is probably due to the uncertainties associated with the low S/N ratio of the data for this transition.

The curvature of the $1 \rightarrow 0$ data is caused by self absorption. A computer program has been written to correct the measured intensities for self absorption. Given estimates for the HCl partial pressure, the temperature and the optical path length X, the computer code calculates the absorption coefficient α_J for each $v = 1 \rightarrow 0$ P-branch transition. The measured intensity $I_s(J)$ is then corrected for optical thickness according to the relationship (Ref. 19)

$$\frac{I_J}{I_J} = \sum_o^\infty (-1)^n \frac{(\alpha_J X)^n}{n!\sqrt{n}}$$

The computer code determines the rotational temperature from these corrected intensities using a least squares fitting technique. The rotational temperature is used to recalculate the absorption coefficients and hence the corrected intensities. The procedure is repeated until the corrected rotational temperature converges.

A typical vibrational distribution for the same data as Fig. 11 is shown in Fig. 12. The vibrational temperature deduced from the low lying transitions is $T_v = 1700^oK$. The actual vibrational state number densities can be calculated from the overall system response. This has been estimated from an average of all the spectral data. Figure 13 shows the vibrational number densities obtained in this manner. The N_o level is calculated from the HCl partial pressure.

Several experiments have been conducted under various operating conditions, including substitution of hydrogen for deuterium and the use of He diluent.

D_2 = 12.7 Torr , HCl = 1.1 Torr

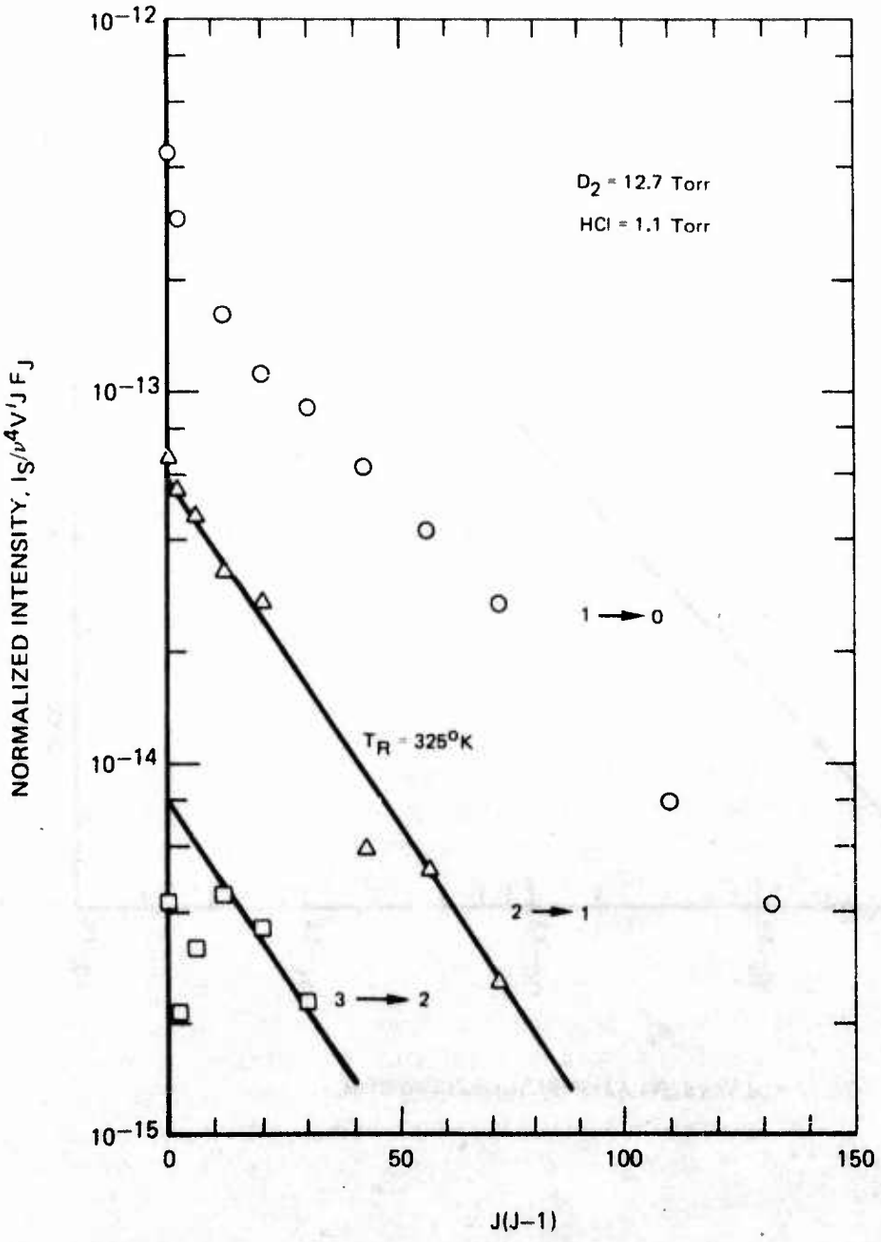

Figure 11. Typical HCl Rotational Distribution

R10-28-3

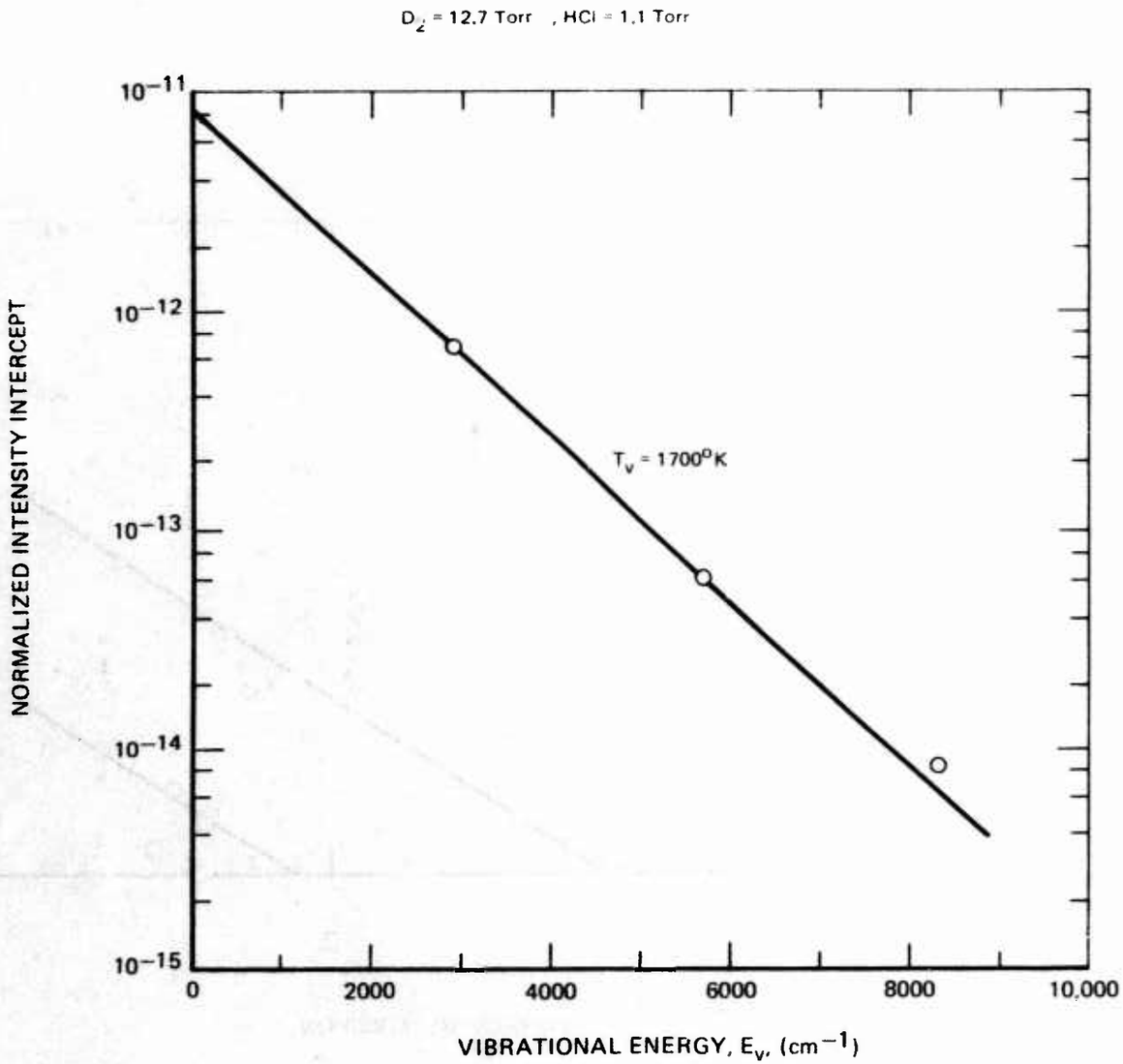

Figure 12. Typical HCl Vibrational Distribution

R10-28-2

D_2 = 12.7 Torr, HCl = 1.1 Torr

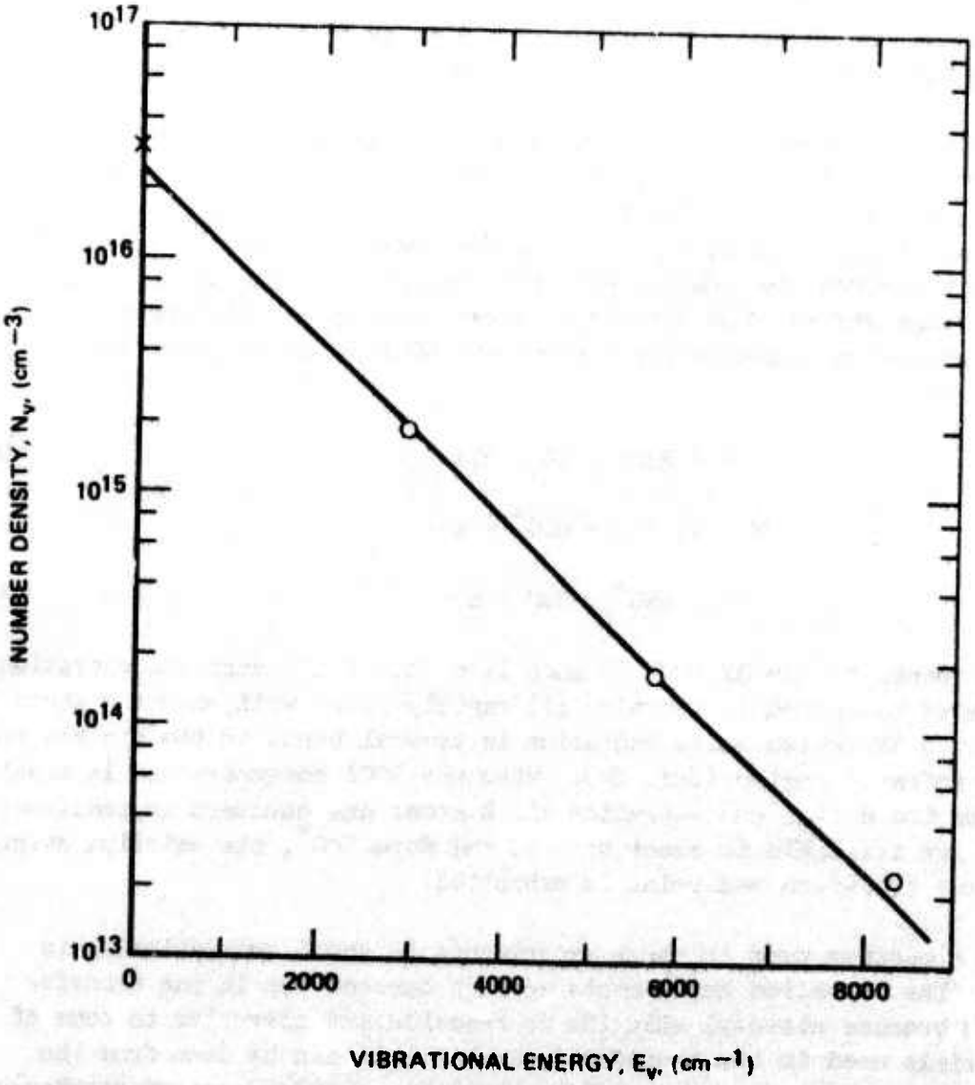

Figure 13. Typical HCl Vibrational Population Distribution

R10-28-4

The emission spectra have been recorded and analyzed according to the above described procedures. The results are given in Table 3.

Measurements to Determine H-Atom Concentration

The optical specific power performance of the D_2-HCl VET laser has been predicted (Ref. 1) to be sensitive to D_2 dissociation. For this reason an attempt was made to determine H-atom concentrations exiting from the standard design electric discharges used in this study. The principal effect of H atoms is to de-excite HCl vibrationally excited molecules (Ref. 20); H atoms are 270 times more effective collision partners than HCl molecules are at 300°K. However, rapid relaxation of $H_2(v)$ has also been measured (Ref. 21); H atoms are 600 times more effective than H_2.

Several techniques have been used to quantitatively determine H-atom concentrations: (1) isothermal calorimeter (Ref. 22), (2) Wrede gage (Ref. 23) and (3) nitrosyl chloride (NOCl) titration (Refs. 24 and 25). The last mentioned technique was chosen for these experiments because it is easier to interpret the results and it is capable of operation in the pressure range wherein the discharge is expected to be maintained. The reaction mechanism sequence for H atoms and NOCl is as follows (Ref. 25):

$$H + NOCl \rightarrow NO + HCl \qquad (1)$$

$$H + NO + M \rightarrow HNO^* + M \qquad (2)$$

$$HNO^* \rightarrow HNO + h\nu \qquad (3)$$

When the concentration of NOCl is much less than the H atom concentration, NO molecules generated in reaction (1) rapidly react with excess H atoms to give excited HNO which emits radiation in several bands in the visible red and near infrared region (Ref. 24). When the NOCl concentration is equal to or exceeds the H atom concentration all H atoms are consumed in reaction (1) and none are available to react with NO and form HNO^*, the emission stops, and a clear titration end point is exhibited.

The apparatus used in these experiments is shown schematically in Fig. 14. The titration experiments weren't carried out in the transfer apparatus because nitrosyl chloride is reactive and corrosive to some of the materials used in the transfer apparatus. As can be seen from the schematic diagram, hydrogen gas flows through a standard design discharge, through a turn in a light trapping elbow, past the nitrosyl chloride mixer and into a 30 cm long, 1.27 cm i.d. flow tube. Nitrosyl chloride and

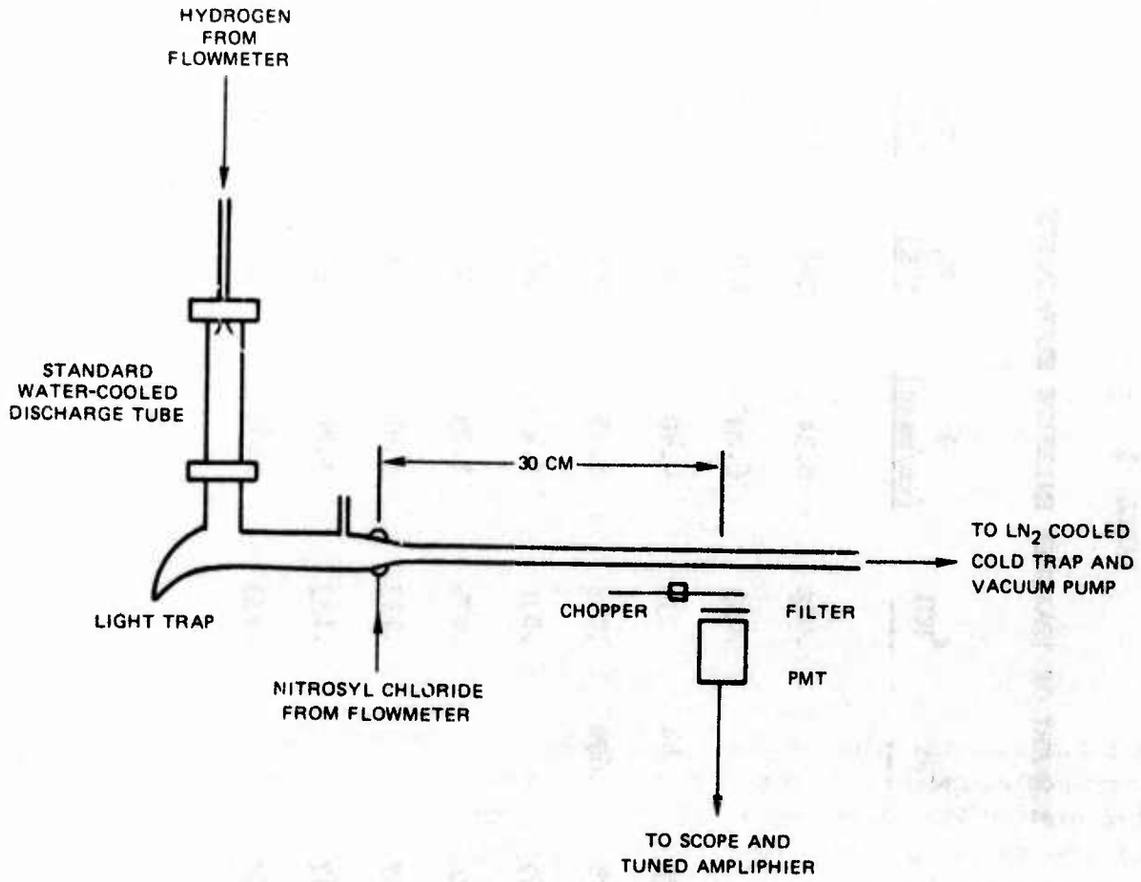

Figure 14. Hydrogen Atom Titration Experiment

76-01-218-1

TABLE 3

SUMMARY OF TRANSFER EMISSION EXPERIMENTS

Run	p (Torr)	X_{H_2}	X_{D_2}	X_{He}	X_{HCl}	$\bar{v}$ (cm/msec)	T_R (°K)	T_V (°K)	T_{V_0} (°K)	P_v (w)	P_{DIS} (w)
1	13.3	.978			.022	6.34	248	1727	1540		
2	12.1	.967			.033	6.22	274	1526	1340		
3	14.0		.422	.544	.034	4.40	240	1600	1420	29	300
4	14.9		.278	.696	.025	5.75	290	1957	1740	479	344
5	11.8		.969		.031	5.49	267	1727	1530	92.0	672
6	13.8		.921		.079	5.93	325	1700	1530	91.1	612
7	14.7		.867		.133	5.43	295	1439	1340	63.0	595
8	14.4		.867		.133	5.86	311	1871	1685	124	525
9	15.7		.867		.133	4.65	235	1655	1515	89.3	540

condensible reaction products are trapped in a liquid nitrogen cold trap, and after an experiment are neutralized in aqueous NaOH. Nitrosyl chloride was used without further purification from cylinders supplied by Matheson. The flowrate of nitrosyl chloride is measured by a rotameter type flowmeter equipped with glass and tantalum floats. Nickel plated fittings and teflon tubing have been used throughout the NOCl supply system. Emission from HNO was detected through the glass flow tube wall by a red sensitive photomultiplier (Hamamatsu R456) equipped with a Wratten 88A filter to block visible emission. The emission was chopped and amplified in a tuned, phase sensitive amplifier (PAR HR-8).

The results have been completely negative with no detectable HNO emission. An estimate of the system sensitivity can be made from the intensity of band emission (Ref. 24), the sensitivity of the PMT (from manufacturer's specifications) and estimates of the collection solid angle and volume. The minimum detectable H-atom concentration can be shown to be:

$$[H]_{min} = 2 \left(\frac{4\pi V_s}{h\nu I_o N_o V_c \Omega_c S R_L}\right)^{1/2}$$

where V_s is the minimum detectable signal voltage, $h\nu$ is the quantum energy of the transition, I_o is band intensity (see Ref. 24), N_o is Avogadro's number, V_c is the collection volume, Ω_c is the collection solid angle, S is the PMT anode sensitivity in A/w and R_L is the PMT load resistor. With $V_s = m\bar{V}$, $V_c = 1\ cm^3$, $\Omega_c/4\pi = .0025$, $R_L = 10^6$ ohms, and $S = 4 \times 10^3$ A/w, the minimum detectable hydrogen atom concentration is $\sim 8 \times 10^{-11}$ mole/cm^3. This corresponds to .03 percent of the typical H_2 concentration.

Several additional experiments were conducted in an attempt to observe emission from HNO*. The discharge tube was operated deliverately far off the experimental design point in order to attempt to maximize H-atom production. Typical pressure in the discharge tube, under these conditions, was 3 Torr and the hydrogen flow was reduced to 1.6 millimoles/sec corresponding to a discharge transit time of approximately 6 msec. The NOCl flowrate was varied over a range of 6 to 210 micromoles/sec corresponding to from 0.3 to 11.5 percent of the hydrogen flowrate. Tests were conducted in which the entering hydrogen stream was allowed to bubble through water in order to saturate the hydrogen stream. The walls of the discharge tube were carefully cleaned and coated with a sulphuric acid. The dc discharge was replaced by a microwave cavity (Ref. 26) enclosing a 1/2 inch o.d. quartz tube which extended down to the mixer when the light trapping elbow was removed. These tests and techniques were tried in succession and in combination with no HNO emission observed.

Several possible explanations of the negative result have been considered. One possible explanation, of course, is that the H atom concentration emanating from the dc discharges is less than the detection limits of the apparatus. NOCl decomposes thermally (Ref. 27) and photochemically (Ref. 28); however, NO is a decomposition product and it should give HNO^* emission. The nitrosyl chloride might be dissociated by back diffusion into the discharge, but again HNO^* should still be seen. A reaction may take place between NOCl and foreign substances in the tube. Finally, quenching of the HNO^* may occur.

If the dissociation fraction were less than 0.03 percent it should have a small effect on laser performance.

Discharge Heat Balance Measurements

The low vibrational temperatures within the donor gas as determined by both the Raman scattering experiment and the transfer/mixing experiments implies that the electric discharges are much less efficient than anticipated (Ref. 1). For this reason, heat balance measurements of the discharges were undertaken. It was decided to conduct these experiments in an apparatus separate from the Raman and transfer experiments in order to facilitate measuring all heat losses. Furthermore, in order to simplify the measurements it was decided to water cool the discharge tube. The discharge tube is identical to standard discharge previously used. The flow tube (length = 38 cm) immediately downstream of the discharge tube expands to a larger diameter $D \approx 5$ cm. Heat losses to the discharge wall, cathode, and this flow tube are individually determined using water calorimeters. The temperature rise across each component is sensed by thermocouples inserted in the cooling water circulating to each component. The water flow rate is measured by a calibrated flowmeter. An injector immediately downstream of the flow tube section can be used to inject a secondary gas into the primary stream. A thermocouple junction is inserted in the flow 11 cm downstream of the injector. Several styles of thermocouples have been used, including a bare thermocouple, a teflon coated thermocouple, and a flow stagnating thermocouple. No meaningful difference in sensible temperature have been noted with the different thermocouple styles. Estimates (Ref. 29) of the average number of collisions that a single molecule being swept past the probe will make with the probe are much less than usual number of collisions required for accomodation of vibrational energy at metallic or teflon surfaces (Ref. 30). Therefore,the temperature measured by this thermocouple probe has been interpreted as representing the gas translational temperature.

Heat balance measurements have been made in nitrogen and hydrogen. Using nitrogen in the discharge it is possible to add CO_2 through the injector, and measure the total power added to the gas. Self relaxation in CO_2 is fast enough to thermalize the mixture. Thus the total power convected

downstream of the flow tube can be determined from the gas translational temperature measured by the thermocouple probe. The results are interesting. In the case of nitrogen 50-60 percent of the discharge power is dissipated through the walls (including the cathode which accounts for 30 percent of the wall losses), 10 percent goes into translation and 30-40 percent is in higher energy states (predominantly vibration). The overall power measured totals approximately 95 percent of the input discharge power. The 30-40 percent of the discharge power attributed to higher energy states is the power which is measured upon injection of the CO_2. At the gas flowrates used, this "vibrational excitation efficiency" corresponds to a power loading of 4.7 to 6.3 kJ/mole which in a Boltzmann vibrational energy distribution corresponds to T_v = 1600-1820°K. These results agree reasonably well with the Raman experiments.

The results of the H_2 discharge heat balance tests are less conclusive. Contrary to the nitrogen discharge results, nearly all of the input discharge power is measured as sensible heat by the thermocouples. Typical values of the fractional discharge power dissipation in various regions of the flow are as follows: discharge tube walls, 30 percent; cathode, 20 percent; flow tube, 20 percent; and 30 percent is sensed as power convected downstream of the flow tube. It appears then that 70 percent of the discharge power is dissipated through the cooled walls, and most of the remaining power is sensed, presumably in translation, downstream of the discharge. Deactivation of vibrational energy at the thermocouple probe appears to be negligible unless the accomodation coefficient for H_2 is markedly higher than that for N_2. The fraction of the discharge power in vibrational energy modes downstream of the discharge implied by these measurements is small; in fact less than the uncertainties (5 percent) in the measurements. The electric discharge coupling efficiency is definitely lower in hydrogen than it is in nitrogen for the conditions explored.

Laser Tests

Attempts have been made to observe stimulated emmission from D_2-HCl in the transfer apparatus. The tests were not successful. For these tests the resonator was comprised of external mirrors with Brewster angle CaF_2 windows. The mirrors used were a silver enhanced silicon total reflecting mirror and a ~ 98 percent reflecting partial transmitter. A liquid nitrogen cooled lead sulfide cell equipped with bandpass filters was used to detect the presence of stimulated emission. Spontaneous emission w observed as confirmed by blocking the mirror farthest from the detector. Wide ranges of flow and

discharge conditions were explored (not all independently) as follows:

D_2 flow	.013 - .038 moles/sec
HCl flow	0 - $\gtrsim$ .001 moles/sec
static pressure	3.5-5 and 6-10 Torr
cavity velocity	10^4 cm/sec and 5×10^3 cm/sec
discharge current	1500-400 Ma (both tube)
discharge voltage	2.3-4.8 kV

Tests were performed with and without zeolite material in the absorbent trap as is indicated by the two pressure ranges and two cavity velocities. Removal of zeolite afforded higher pumping capacities.

Spontaneous emission was not spectrally resolved during these tests so exact information is not available as to vibrational state populations; however, it is suspected that negative results are caused by low inversion densities.

SECTION IV

CONCEPTUAL DESIGN

A preliminary screening has been conducted of vibrational energy transfer (VET) candidate molecular pairs in order to determine their potential for airborne infrared laser system applications. The D_2-HCl system has been selected as most promising based on atmospheric transmission characteristics, cycle configuration, system potential size and weight, and aircraft compatibility. The electric discharge VET approach appears to offer higher potential for airborne applications than thermal or chemical VET excitation. Preliminary VET laser performance calculations indicate that maximum performance may require a low gas temperature within the active medium. Previous investigation (Ref. 31) has shown that the most effective means of cooling subsonic flow laser mixtures is by a liquid N_2 heat exchanger. This technique is being explored in the present investigation. Reconfirmation of these estimates is required when additional analytical and/or experimental data become available.

SECTION V

DISCUSSION OF RESULTS AND CONCLUSIONS

Measurements have been made of the vibrational excitation of hydrogen downstream of an electric discharge. Measurements have also been made of the vibrational excitation of hydrogen chloride as a result of mixing with discharge excited deuterium (and hydrogen). A relationship between the measured HCl vibrational temperature and the corresponding D_2 vibrational temperature can be derived from a consideration of the VV transfer reaction

$$D_2(v=1) + HCl(v=0) \rightleftharpoons D_2(v=0) + HCl(v=1) + \Delta E.$$

The rate constants are the same as defined previously and ΔE is the energy defect. As discussed above the mixing D_2 and HCl streams, in the transfer apparatus, rapidly reach a mutual vibrational equilibrium in a time comparable to the VV transfer time. At equilibrium, the vibrational temperature of deuterium, T_{v_2}, is related to the HCl vibrational temperature, T_{v_1} by detailed balance. Using Boltzmann factors to describe the vibrational excitation it can be shown that

$$\frac{\theta_1}{T_{v_1}} - \frac{\theta_2}{T_{v_2}} = \frac{\Delta E}{kT},$$

where θ_1 and θ_2 are the characteristic vibrational temperatures ($\theta = G(1)\, hc/k$) of HCl and D_2, respectively. Since $\Delta E/k = \theta_2 - \theta_1$, this expression can be written

$$T_{v_2} = \frac{T_{v_1}\theta_2}{\theta_1 - (\theta_1 - \theta_2)\frac{T_v}{T}}$$

This equation shows that at equilibrium the vibrational temperature of D_2 is less than HCl temperature.

An estimate of the initial deuterium vibrational temperature, i.e., prior to mixing, can be made from the equilibrium vibrational temperature by assuming that ther is no loss of vibrational quanta during VV equilibration. This is a valid assumption if VV energy transfer is much faster than VT relaxation, as is usually the case. The conservation of vibrational quanta can be written

$$N_2 \sum_v v \exp\left[\frac{-hcG_2(v)}{kT_{v_2}}\right]_{\text{initial}} = N_2 \sum_v v \exp\left[\frac{-hcG_2(v)}{kT_{v_2}}\right]_{\text{equil}}$$

$$+N_1 \sum_v v \exp\left[\frac{-hcG_1(v)}{kT_{v_1}}\right]_{\text{equil}}$$

where $G_2(v)$ and $G_1(v)$ are vibrational energies of level v referred to the ground vibrational state of D_2 and HCl respectively, and N_2 and N_1 are the number densities of D_2 and HCl respectively. The initial deuterium vibrational temperatures, T_{v_o}, deduced in this manner are shown in Table 3.

The power convected out of the discharge in the vibrationally hot deuterium flow was calculated from T_{v_o} and the known flowrates. The discharge power input was calculated from the discharge voltage (across the electrodes) multiplied by the discharge current. Note that in run number 5 only one discharge tube, the one closest to the spectrometer, was activated. The numbers shown are applicable to the two discharge tubes activated and, therefore, are comparable to the other data in this table.

The data of Table 3 tend to indicate that it may be that the discharge is inefficiently coupled to the gas vibrational modes. If a correction is made for the estimated power going into the cathode fall, the estimated fractional power transfer to vibration is 20-25 percent. These results are somewhat questionable due to the indication of rapid decay of HCl vibrational excitation. However, it should be noted that the Raman experiments support the transfer experimental results, in that a low degree of vibrational excitation is indicated. The transfer experiments indicate T_{v_o} = 1300-1700°K while the Raman scattering tests indicate T_{v_o} = 1000-1350°K.

The low measured donor gas excitation can't be soley attributed to inefficient discharge coupling at this time. Another possible explanation is that the vibrational excitation is adequate, however, vibration deactivation rapidly thermalizes the excitation in the time that it takes for the discharge donor gas to flow from the discharge to the region of excitation measurement. If this latter explanation is the dominant effect then since the Raman experiments show low vibrational temperatures rapid vibrational excitation of the deuterium itself must be considered.

The results of several Raman scattering experiments are shown in Table 4. The efficiency of discharge in converting electrical energy to vibrational energy in the gas has been calculated from the Raman determinations and the electrical power input. The vibrational energy per mole is calculated assuming that the measured vibrational temperature is valid for all levels

TABLE 4

SUMMARY OF RAMAN EXPERIMENTS

WITH ELECTRIC DISCHARGE EXCITED GASES

Nitrogen	14 Torr	Sonic Tube		$\dot{n}$ = .013 mole/sec	
i_d (mA)	V_d (V)	P_{DIS} (w)	T_v (^oK)	$E_v(T_v)$ (kJ/mole)	η (%)
30	2150	64.5	1360	2.8	56
60	2000	120	1558	4.2	44
75	1850	139	2000	8.0	74

Hydrogen	20 Torr	Sonic Tube		$\dot{n}$ = .030 mole/sec	
i_d (mA)	V_d (V)	P_{DIS} (w)	T_v (^oK)	$E_v(T_v)$ (kJ/mole)	η (%)
30	2300	69	926	0.08	3.5
60	2150	129	1080	0.20	4.7
90	2000	180	1142	0.27	4.5

Hydrogen	21 Torr	Radial Injector		$\dot{n}$ = .030 mole/sec	
i_d (mA)	V_d (V)	P_{DIS} (w)	T_v (^oK)	$E_v(T_v)$ (kJ/mole)	η (%)
30	3900	117	1200	0.35	8.9
30	3900	117	1310	0.54	13.8

up the vibrational ladder. It is noted that the nitrogen measurements, at least at the higher discharge current, are quite reasonable in comparison to theoretical predictions. The efficiency in hydrogen is quite low.

These results can be compared with other previous investigations. There are only a limited number of direct measurements of vibrational excitation from electric discharges. Nelson et al (Ref. 32) used Raman scattering to determine vibrational excitation in N_2 15 cm downstream of a transformer excited discharge. They found a vibrational temperature $T_v = 1950^oK$. In later measurements on a similar N_2 discharge in the pressure range p = 100-150 Barrett and Harvey, using a Fabry-Perot interferometric Raman technique, were able to determine $T_v = 1930\text{-}2356^oK$ (Ref. 33). The only published previous measurement of vibrational excitation in a hydrogen discharge utilized vacuum UV absorption of vibrational states (Ref. 34) at 3 Torr pressure excited in a microwave discharge. The workers in this study estimated that 1-4 percent of the hydrogen was vibrationally excited. This corresponds to $T_v = 1300\text{-}1900^oK$.

The Raman scattering measurements of vibrational excitation reported herein are in agreement with the broad range of previous determinations. In both N_2 and H_2 they are on the low side of these previous measurements. This may be indicative of some particular inefficiency associated with the present discharges.

The heat balance measurements discussed in the previous section bear out the conclusion that the present discharges are characterized by low vibrational excitation efficiencies. The discharge efficiencies estimated from the Raman experiments are in good agreement with the heat balance measurements. The very low discharge efficiency indicated by the Raman measurements in hydrogen is within the experimental errors that are expected from the heat balance measurements. It is therefore not surprising that negligible efficiency is implied from those experiments.

No definite conclusions can be drawn as to the reasons for the low discharge efficiencies. It appears at the present time that deactivation by atomic hydrogen doesn't account for the low efficiencies. The modeling calculations indicate that although some deactivation occurs, even at the low atom concentrations predicted (.0016 percent) the decrease in vibrational temperature (less than 10 percent) is not nearly enough to give the low efficiencies observed, unless the efficiency was low to begin with at the exit of the discharge. The nitrosyl chloride titration experiments indicate that the atomic concentrations issuing from the standard discharges is less than the sensitivity of the experiment ($\sim$ .03 percent). Although the tiration experiment is not sensitive enough to confirm the predicted concentrations, it should be sensitive enough to measure atomic concentration levels which would be deleterious to laser power extraction.

The higher heat losses to the wall measured with hydrogen compared to nitrogen may reflect the higher thermal diffusivity. Some inefficiencies are naturally expected because of the strong cooling. Additional inefficiency is expected because of the short discharge tubes (to minimize H-atom production) and the relatively higher ratio of cathode potential fall compared to the total voltage.

The present study has answered several important questions concerning the generation of stimulated emission by vibrational energy transfer in the D_2-HCl system. Key questions remain concerning the exact nature and cause of the low discharge efficiency in producing vibrational excited molecules. Whether the inefficiency can be overcome by brute force, i.e., increased power loading, or more sophisticated techniques, has yet to be determined. Increased testing and combination of tests such as the Raman scattering experiment and heat balance measurements will answer these questions.

Numerical calculations have been made to simulate the Raman scattering measurements of post discharge hydrogen vibrational excitation. Particular attention was paid to the evolution of the hydrogen vibrational levels through the 12 cm discharge region and the 19 cm downstream of the discharge exit. This corresponds to the position where the Argon ion laser beam is focused into the hydrogen afterglow.

Calculations made previously of the electron energy distribution in a uniform discharge (Ref. 1), give the electron excitation and dissociation rates, average electron energy and drift velocity as functions of the Townsend parameter. These rates are used along with models of vibrational-vibration energy transfer and vibrational-translation relaxation by molecular and atomic hydrogen. The buildup of $H_2(v)$ is calculated in this manner through the discharge. At the discharge exit the electron collision rates are set equal to zero and calculation is carried downstream.

Computations have been made simulating the nominal discharge conditions maintained in the Raman scattering experiments, i.e.: $p = 20$ Torr, $E/n = 2.5 \times 10^{-15}$ V-cm^2, $i = 55$ mA, $v = 5 \times 10^3$ cm/sec and $T_i = 300^\circ$K. The effect of discharge current has been examined by varying the discharge power density, P/V. Figure 15 shows the evolution of the effective hydrogen vibrational temperature between the ground and the first excited vibrational level for several values of the discharge power density parameter. The nominal experimental discharge current, $i = 55$ mA corresponds to a power loading of $P/V = 1.7$ w/cm^3. The effective vibrational temperature rises rapdily until the end of the discharge then decays at a rate depending on the power loading. The decay of vibrational excitation is mainly due to VT decay by H atoms. Higher power loading leads to higher atom concentrations

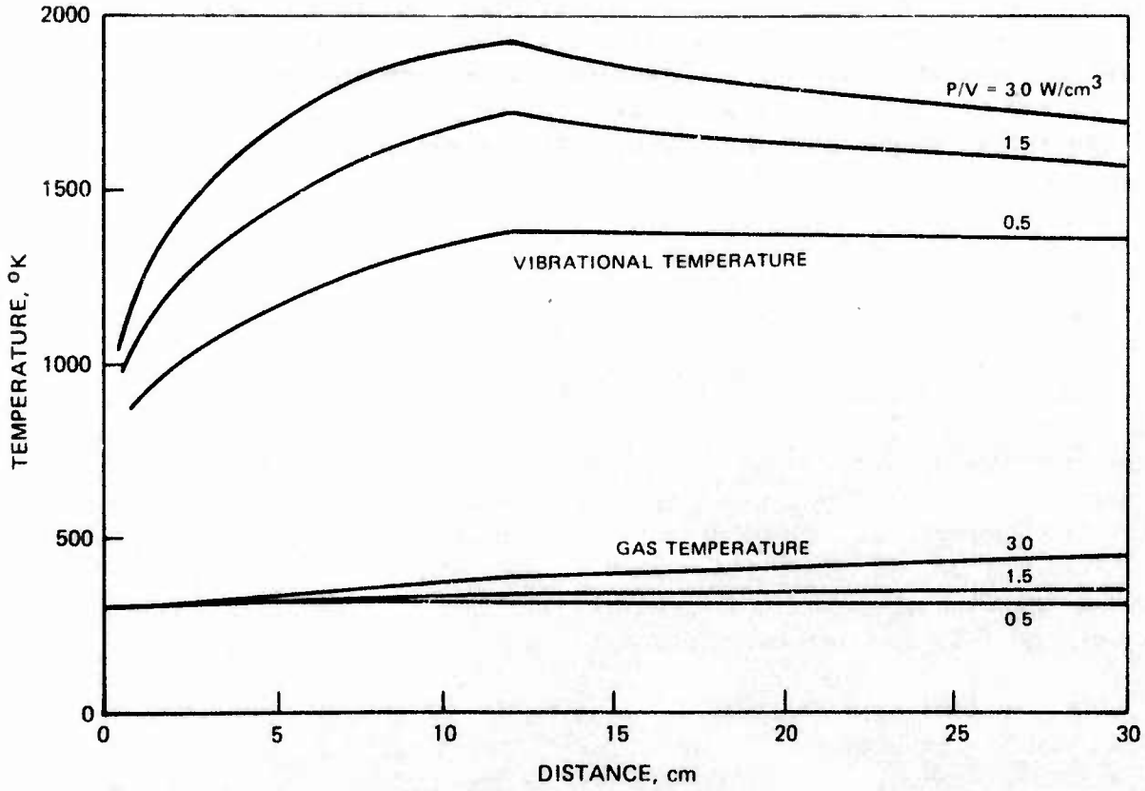

Figure 15. Hydrogen Discharge/Afterglow Excitation Profiles

76-01-240-1

at the discharge exit. The H-atom concentration at the discharge exit is predicted to be $\sim 10^{13}$ cm^{-3}, corresponding to a mole fraction of 1.6×10^{-3} percent, for P/V = 1.7 w/cm^3.

The evolution of the hydrogen vibrational distribution is shown in Fig. 16 for a low power loading parameter. It can be seen that the effect of the large vibrational anharmonicity in hydrogen mainly affects the vibrational levels higher than the fourth. The behavior of the lower levels is governed mainly by BT energy transfer through atomic collisions.

Calculations have been made down to quite low discharge power loading densities in order to simulate the possible effect of large discharge inefficiencies described in the section on discharge heat balance measurements. It should be noted for P/V = 0.5 w/cm^3, typical of inefficient discharge couplings measured, the first vibrational level temperature rises to 1390°K at the end of the discharge and falls to 1360°K at 30 cm. These values are in general agreement with the experimental results.

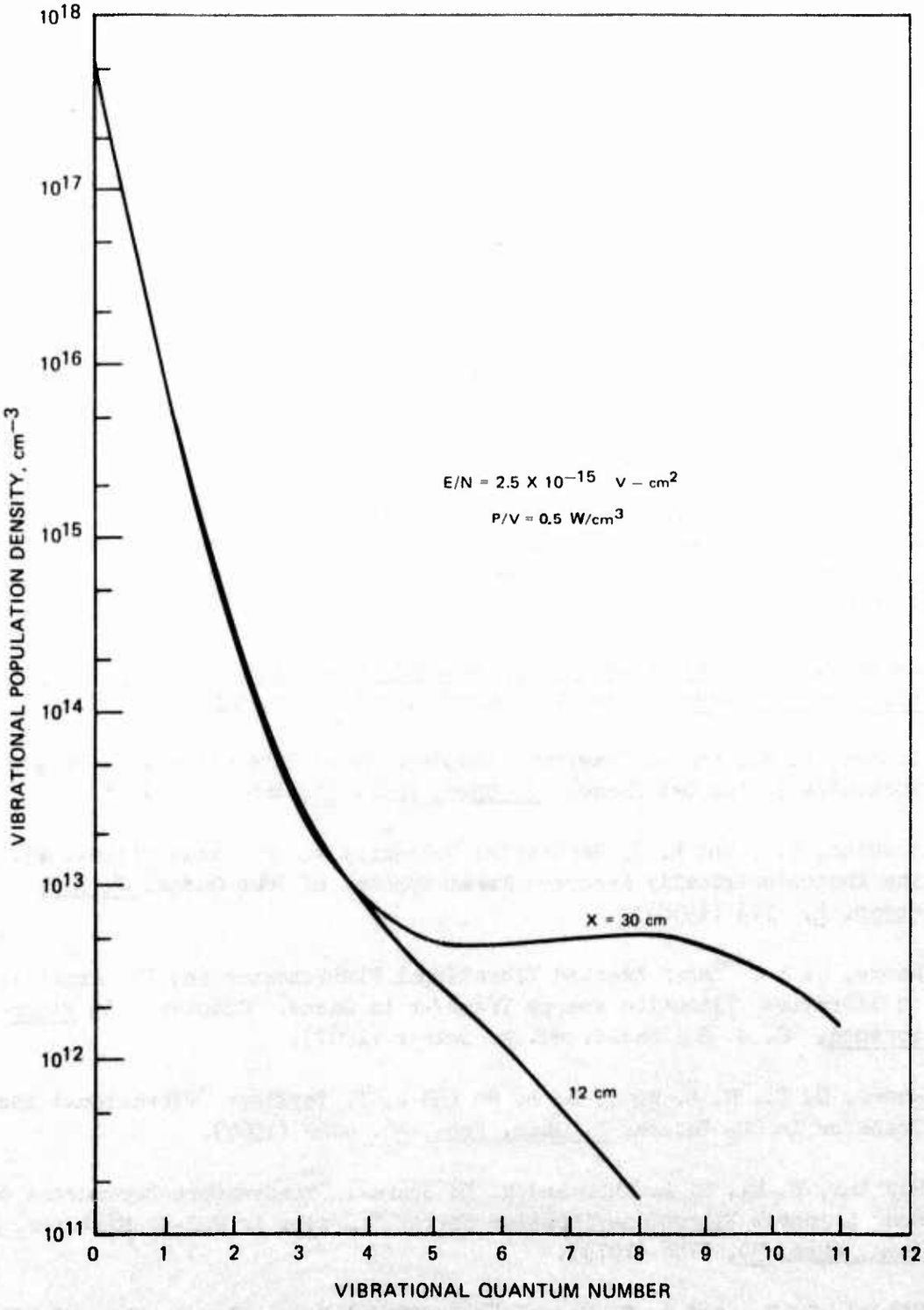

Figure 16. Evolution of Hydrogen Vibrational Distribution

76-01-240-2

REFERENCES

1. UARL Proposal P-N293: Proposal to Investigate a 3-5 Micron VET Laser. September 1974.

2. Pivovsky, M., and M. R. Nagel: Tables of Blackbody Radiation Functions. MacMillan Co., New York (1961).

3. Lochte-Holtgreven, W.: Plasma Diagnostics. North Holland Publishing Co. Amsterdam (1961).

4. Fouche, D. G., and R. K. Chang: "Relative Raman Cross Section for O_3, CH_4, C_3H_8, NO, N_2O, and H_2". Appl. Phys. Lett. 20, 256 (1972).

5. Rudder, R. R., and D. R. Bach: Rayleigh Scattering of Ruby Laser Light By Neutral Gases. J. Opt. Soc. AM. 58, 1260 (1968).

6. Black, G., R. L. Sharpless and T. G. Slanger: "Measurements of Vibrationally Excited Molecules by Raman Scattering. I. The Yield of Vibrationally Excited Nitrogen in the Reaction N + NO N_2 + O". J. Chem. Phys. 58, 4792 (1973).

7. Herzberg, G.: Molecular Spectra and Molecular Structure. I. Spectra of Diatomic Molecules. D. Van Nostrand Co., Princeton, New Jersey (1950).

8. Golden, D. M., and B. Crawford: "Absolute Raman Intensities, I. Method for Molecules in the Gas Phase". J. Chem. Phys. 36, 1654 (1962).

9. Yoshino, T. , and H. J. Bernstein: "Intensity in the Raman Effect. VI. The Photoelectrically Recorded Raman Spectra of Some Gases". J. Mol. Spect. 2, 213 (1958).

10. Moore, C. B.: "Laser Excited Vibrational Fluorescence and Its Application to Vibration Vibration Energy Transfer in Gases". Chapter 3 in Fluorescence, G. G. Guilbault, ed. M. Dekker (1967).

11. Moore, C. B., R. E. Wood, B. L. Hu and J. T. Yardley: "Vibrational Energy Transfer in CO_2 Lasers". J. Chem. Phys. 46, 4222 (1967).

12. Hopkins, B. M., H. L. Chen and R. D. Sharma: "Temperature Dependence of Near Resonant Vibration-Vibration Energy Transfer in HCl-D_2 Mixtures". J. Chem. Phys. 59, 5758 (1973).

13. Zittel, P. F., and C. B. Moore: "Vibrational Relaxation in HBr and HCl from 144°K to 584°K". J. Chem. Phys. 59 6636 (1973).

REFERENCES (Cont'd.)

14. Lukasik, J. and J. Ducuing: "Vibrational Relaxation of Deuterium at 300°K." J. Chem. Phys, 60, 331 (1973).

15. Hirschfelder, J. O., C. F. Curtiss and R. B. Bird: "Molecular Theory of Gases and Liquids." John Wiley, New York (1964).

16. UARL Proposal P-N293. Loc. Cit. Appendix C.

17. Benedict, W. S., R. Herman, G. E. Moore and S. Silverman: "Infrared Line and Band Strengths and Dipole Moment Function in HCl and DCl." J. Chem. Phys. 26, 1671 (1957).

18. Toth, R. A., R. H. Hunt and E. K. Plyler: "Line Strengths, Line Widths and Dipole Moment Function for HCl." J. Mol. Spec. 35, 110 (1970).

19. Mitchell, A. C. G. and M. W. Zemansky: Resonance Radiation and Excited Atoms. Cambridge University Press, London (1934).

20. Arnoldi, D. and J. Wolfrum: "The Reaction of Vibrationally Excited HCl with Oxygen and Hydrogen Atoms." Chem. Phys. Lett. 24, 234 (1974).

21. Heidner, R. F., III, and J. V. V. Kasper: "An Experimental Rate Constant for H. + H_2 (" = 0)". Chem. Phys. Lett. 15, 179 (1972).

22. Tollefson, E. L. and D. J. LeRoy: "The Reaction of Atomic Hydrogen with Acetylene." J. Chem. Phys. 16, 1057 (1948).

23. Greaves, J. C. and J. W. Linnett: "Recombination of Atoms at Surfaces." Trans. Farad, Soc. 55, 1338 (1959).

24. Clyne, M. A. A. and B. A. Thrush: "Mechanism of Chemiluminescent Reactions Involving Nitric Oxide -- The H + NO Reaction." Discuss, Faraday Soc. 33, 139 (1962).

25. Clyne, M. A. A. and D. H. Stedman: "Reactions of Atomic Hydrogen Chloride and Nitrosyl Chloride." Trans. Faraday Soc. 62, 2164 (1966).

26. Fehsenfeld, F. C., K. M. Evenson and H. P. Broida: "Microwave Discharge Cavities Operating at 2450 MHz." Rev. Sci. Instrum., 36, 294 (1965).

27. Waddington, G., and R. C. Tolman: "The Thermal Decomposition of Nitrosyl Chloride." J. Amer. Chem. Soc., 57, 689 (1935).

28. Goodeve, C. F. andS. Katz: "The Absorption Spectrum of Nitrosyl Chloride." Proc. R. Soc. Lond. 172, 342 (1939).

29. At the pressures of interest here it can be shown that the average number of collisions a single molecule will make with the probe is given by $(N) = \frac{1}{4} vA/uA_s$, where v is the mean thermal speed, A is the area of the probe, u is the mean flow velocity and A_s is the swept area of the probe. Under typical experimental conditions (N) = 18 collisions.

30. Black, G., H. Wise, S. Schechter and R. L. Sharpless: "Measurements of Vibrationally Excited Molecules by Raman Scattering. II. Surface Deactivation of Vibrationally Excited N_2." J. Chem. Phys. 60, 3526, (1974) and referenced cited therein.

31. Eckbreth, A. C., et al: "Conceptual Design Studies of CO Electric Discharge Laser Systems." AFWL Contract No. F29601-73-C-0027, Final Report AFWL-TR-73-187, August 1973.

32. Nelson, L. Y., A. W. Saunders, Jr., A. B. Harvey and G. O. Neely: "Detection of Vibrationally Excited Homonuclear Diatomic Molecules by Raman Spectroscopy." J. Chem. Phys. 55, 5127 (1971).

33. Barrett, J. J. and A. B. Harvey: "Vibrational and Rotational-Translational Temperatures in N_2 by Interferometric Measurement of the Pure Rotational Raman Effect." J. Opt. Soc. Amer. 65, 392 (1975).

34. Heidner, R. F. and J. V. V. Kasper: "Observation of Vibrationally Excited H_2 In Active Hydrogen." J. Chem. Phys. 51, 4163 (1969).

☆ U. S. GOVERNMENT PRINTING OFFICE: 1976 — 657-630/1076